Can scalable design of wings for flapping wing micro air vehicle be inspired by natural flyers?

Nan, Yanghai; Peng, Bei; Chen, Yi; Feng, Zhenyu; McGlinchey, Don

Published in:
International Journal of Aerospace Engineering

DOI:
10.1155/2018/9538328

Publication date:
2018

Document Version
Publisher's PDF, also known as Version of record

Hindawi
International Journal of Aerospace Engineering
Volume 2018, Article ID 9538328, 24 pages
https://doi.org/10.1155/2018/9538328

Research Article

Can Scalable Design of Wings for Flapping Wing Micro Air Vehicle Be Inspired by Natural Flyers?

Yanghai Nan,[1,2,3,4] **Bei Peng**,[1,2,3] **Yi Chen**,[1,2,3,4] **Zhenyu Feng**,[1,2] **and Don McGlinchey**[4]

[1]*School of Mechanical and Electrical Engineering, University of Electronic Science and Technology of China, Chengdu 611731, China*
[2]*Center for Robotics, University of Electronic Science and Technology of China, Chengdu 611731, China*
[3]*Sichuan Artigent Robotics Equipment Co., Ltd, Chengdu 610213, China*
[4]*School of Engineering and Built Environment, Glasgow Caledonian University, Glasgow G4 0BA, UK*

Correspondence should be addressed to Bei Peng; beipeng@uestc.edu.cn

Received 21 April 2018; Accepted 6 August 2018; Published 21 October 2018

Academic Editor: Hikmat Asadov

Lift production is constantly a great challenge for flapping wing micro air vehicles (MAVs). Designing a workable wing, therefore, plays an essential role. Dimensional analysis is an effective and valuable tool in studying the biomechanics of flyers. In this paper, geometric similarity study is firstly presented. Then, the p_w − AR ratio is defined and employed in wing performance estimation before the lumped parameter is induced and utilized in wing design. Comprehensive scaling laws on relation of wing performances for natural flyers are next investigated and developed via statistical analysis before being utilized to examine the wing design. Through geometric similarity study and statistical analysis, the results show that the aspect ratio and lumped parameter are independent on mass, and the lumped parameter is inversely proportional to the aspect ratio. The lumped parameters and aspect ratio of flapping wing MAVs correspond to the range of wing performances of natural flyers. Also, the wing performances of existing flapping wing MAVs are examined and follow the scaling laws. Last, the manufactured wings of the flapping wing MAVs are summarized. Our results will, therefore, provide a simple but powerful guideline for biologists and engineers who study the morphology of natural flyers and design flapping wing MAVs.

1. Introduction

Over the last decade, numbers of scholars have explored and studied flapping wing MAVs inspired by natural flyers, such as insect-like MAVs (i.e., Micromechanical flying insects [1], Harvard RoboBee [2], KUBeetle [3], DelFly [4], FlowerFly [5], Festo-Dragonfly [6], and Festo-Butterfly [7]) and bird-like MAVs (i.e., Nano hummingbird [8], Giant hummingbird [9, 10], and Festo-SmartBird [11]) since natural flyers have surprising behaviours including flapping, gliding, and soaring. In particular, flies, bees, and hummingbirds are characterized by acrobatic hovering flight. However, generating enough lift is a constant challenge in designing flapping wing MAVs, which mostly relies on wing performances such as flapping frequency, wing surface, aspect ratio, flapping amplitude, lift coefficient, and wing loading. Therefore, wing design remains a challenging task.

For such reason, wing design has become a major research topic over the last decade. In nature, flying animals have widely different shapes, configurations, and structural properties, which may be linked to the differences in flapping kinematics [12]. Several flat and rigid wings were designed, studied, and optimized by some researchers. For example, Ansari et al. [13] studied the effects of different wing geometries based on the unsteady aerodynamic numerical analysis. Results showed that the best performing wing should have nearly straight leading edges with large surfaces outboard. Phillips et al. [14] presented recent experimental results on rigid rectangular wings, and they observed that the wing with AR = 12 generated the highest lift coefficient. Besides, rigid hawkmoth-like wings are also studied by Lua et al. [15]. Although certain results were obtained on rigid flat wings, rigid wings had worse performance than flexible wings [16–19]. Natural flyers have wings with several degrees of

freedom when flapping. They can vary from one flight mode to another by adjusting the wing motion pattern with the wing shape deformation [16, 20]. It means that natural flyers flex their wings actively or passively to change the shape, geometry, and surface of the wing when flapping. The increase in the projected wing area enhances the aerodynamic performance when wing deformation occurs [21]. Additionally, Nan et al. [22] studied the flexible wings with a camber angle. The result shows that the camber angle and aspect ratio specifically have a significant effect on the force generation and wing efficiency. At the same time, the aspect ratio effects are further studied on revolving with Rossby number [23]. To obtain the rapid predictions of lift generation, an improved quasi-steady aerodynamic model for flapping wings during hovering was also proposed [24]. Recently, the optimization study on simple and complex pitching motions for flapping wing over hovering is done by Lee and Lua [25].

Although plentiful researches have been launched such as [26, 27], no standard criteria are presented, as wing design of flapping wing MAVs is strongly varied with diverse categories of flapping wing MAVs. Therefore, scaling law is necessary and useful as a basic tool in supervising wing design. By studying the effects of different physical parameters on flight performance, it will benefit for the research of flying animals' flight mechanisms, which will then help to discover the pattern applied in designing flapping wing MAVs. By means of analyzing the scaling study, it essentially indicates the relation among different physical parameters in different species or the same species [28]. Importantly, it can be employed to estimate a parameter varying with another one, which is a significantly efficient tool in designing flapping wing MAVs. Some scholars studied and explored the relation between wing characteristics and body mass from a natural perspective, which is applied in the wing design of bioinspired flapping wing MAVs. Dudley [29] studied the relations between morphometrics and kinematics of butterflies. Byrne et al. [30] presented the relationship among wing loading, wingbeat frequency, and body mass on homopterous insects. Corben [31] exhibited the relation among wingbeat frequency, wing area, and mass of flying insects and hummingbirds, while Bullen and McKenzie [32] explored the scaling law between wingbeat frequency and amplitude angle on bats. Ha et al. [33] studied the relationship between wingbeat frequency and resonant frequency of the wings on insects. Greenewalt [34] also surveyed the relationship between wing length and weight of natural flyers. Tennekes [35] presented the relations among different physical parameters for different flyers including insects, birds, and even jets. Besides, Shyy et al. [36] did a similar study as well, and a simple summary of the relation among different physical parameters was presented.

Although many studies on natural wing characteristics have been conducted, no comprehensive analysis regarding these characteristics is systematically organized, especially for the wing lumped parameter k of flying animals. Besides, comparative studies on flapping wing MAVs have not been accomplished. In this study, the geometric similarity study is firstly explored and then the $p_w - \mathrm{AR}$ ratio is presented and employed to estimate the wing performances. The comprehensive scaling laws are subsequently analyzed and achieved from a morphometric perspective by collecting extensive data of natural flyers. The wing performances of the existing flapping wing MAVs are also studied, which follows the obtained scaling laws. Last, the steps of wing manufacture and take-off demonstration are presented, and the manufactured wings of the flapping wing MAVs are summarized.

2. Basic Definitions and Geometric Similarity

This section presents the flying animals and flapping wing MAVs that are assessed in this study. Some parameters are collected from existing literature, whereas others are computed based on theoretical functions provided in this paper. The units and definitions of parameters are unified to make the results comparable. Some morphological parameters of natural flyers from existing literature are exhibited in Table 1. The collected species of flying animals include insects (such as bees, mosquitoes, flies, beetles, dragonflies, butterflies, and hawkmoths), bats, hummingbirds, and other birds such as seabirds.

If birds are assumed to be a geometric similarity, then the weight, lift force, and mass can be expressed as characteristic length l during steady-state flight. The total surface A including two wings' surface or four wings' surface with the body area projected, and volume V varies with characteristic length l, that is, $A \sim l^2$, $V \sim l^3$. In hovering or steady-state flight, it is reasonable to assume that the weight is proportional to lift force $\bar{F}_L$.

$$W \sim \overline{F}_L \sim \frac{1}{2} C_L \rho V_t^2 A, \tag{1}$$

where W is weight (N), ρ is air density (kg/m^3), C_L is lift coefficient, and V_t is forward flight velocity (m/s).

$$W = mg \sim \bar{F}_L \sim V \sim l^3, \tag{2}$$

where m is the mass of flyer (kg) and g is the gravitational acceleration (m/s^2).

Total surface can be presented as

$$A \sim l^2 \approx \left(m^{1/3}\right)^2 \approx m^{2/3}, \tag{3}$$

where A is the total surface (mm^2), including two wings' surface or four wings' surface with the body area projected.

2.1. Mean Wing Chord. The mean wing chord is defined as a single wing surface divided by the wing length, which is expressed as follows:

$$\bar{c} = \frac{S}{R} \sim l \sim m^{1/3}, \tag{4}$$

where S is the single wing surface (mm^2) and R is the single wing length (mm).

Table 1: Wing parameters of various natural flyers.

Species		m (g)	R (mm)	f (Hz)	S (mm^2)	p_w (N/m^2)	AR	k
Brachycera (fly)	Hoverfly [59]	0.022	11.3	166	—	—	—	—
	[60]	0.027	9.3	160	20.48	6.53	8.45	0.44
	Fruit fly [61]	0.001	2.8	225	—	—	—	—
	[60]	0.00072	2.02	254	1.36	2.59	6	0.28
	[52]	0.002	3	200	1.45	6.76	12.41	0.14
	March fly [62]	0.065	17	100	—	—	—	—
		0.027	14	130	—	—	—	—
	Conopid fly [62]	0.027	12	144	—	—	—	—
	Bluebottle fly [62]	0.062	10	135	—	—	—	—
	Black fly [62]	0.0008	3.8	183	—		—	—
	Drone fly [60]	0.068	11.4	157	36.89	9.09	7.05	0.49
		0.17	14.7	209	—	—	—	—
	Calliphiora [63]	0.015	—	180	15.3	4.80	—	0.5
		0.094	—	156	39.8	11.57	—	0.45
		0.062	—	165	33.85	8.97	—	0.5
		0.106	—	156	36.55	14.21	—	0.39
		0.061	—	161	30.55	9.78	—	0.44
		0.064	—	152	30.55	10.27	—	0.41
		0.035	—	156	25.3	6.78	—	0.47
		0.033	—	165	26.25	6.16	—	0.53
		0.03	—	161	28.5	5.16	—	0.59
		0.044	—	165	29	7.43	—	0.5
		0.05	—	175	33.65	7.28	—	0.58
	Eristalis [63]	0.206	—	185	49.4	20.43	—	0.46
		0.106	—	175	38.25	13.58	—	0.46
		0.093	—	180	41.95	10.86	—	0.55
		0.176	—	185	43.95	19.62	—	0.43
		0.143	—	185	40.95	17.11	—	0.44
Nematocera (Mosquite)	Crane fly [60]	0.011	12.7	45.5	30.18	1.85	10.69	0.29
	[45]	0.05	18.1	58	—	—	—	—
	Aedes aegypti [64]	0.0012	4.4	470	—	—	—	—
	Aedes aegypti [65]	0.001	2.5	600	1.75	2.8	7.14	0.74
	Tipulasp [63]	0.028	17.3	53	79.58	1.72	7.52	0.56
	Theobaldia annulata [63]	0.01	6.3	262	10.08	4.86	7.88	0.58
	Nematocera [63]	0.021	—	63	37.75	2.73	—	0.36
		0.035	—	42	69	2.49	—	0.34
		0.03	—	63	43.95	3.34	—	0.35
		0.034	—	49	62.5	2.67	—	0.37
		0.03	—	49	65	2.26	—	0.41
		0.021	—	49	45.35	2.27	—	0.34
		0.02	—	63	30.7	3.19	—	0.3
		0.075	—	49	76	4.84	—	0.3
		0.023	—	48	65.5	1.72	—	0.46
		0.022	—	48	60	1.80	—	0.43
		0.022	—	48	53	2.03	—	0.38
		0.025	—	49	50.5	2.43	—	0.35
		0.001565	—	67	10.65	0.72	—	0.4
		0.00083	—	80	9	0.45	—	0.55

Table 1: Continued.

Species		m (g)	R (mm)	f (Hz)	S (mm^2)	p_w (N/m^2)	AR	k
		0.0099	—	262	8.45	5.74	—	0.49
		0.001025	—	600	1.2	4.19	—	0.5
		0.00189	—	360	2.5	3.70	—	0.46
		0.0058	—	277	7.5	3.79	—	0.6
	Orchid bee [66]	0.09	10	214	—	—	—	—
	[52]	0.15	13	189	—	—	—	—
	[63]	0.82	25	105	—	—	—	—
	Honey bee [45]	0.1	9.8	197	30.14	16.6	6.4	0.42
	Honey bee [67]	0.1	15.9	197	—	—	—	—
	Bumble bee [60]	0.18	13.2	155	54.9	15.6	6.35	0.44
	[68]	0.6	22.3	167	—	—	—	—
	[67]	0.23	20.7	152	—	—	—	—
	[67]	0.23	20.7	140	—	—	—	—
	Xylocopa pubescens [33]	0.66	10	111.1	63.7	25.53	3.14	0.39
		0.72	9.65	111.1	59	29.91	3.16	0.34
	Bombus rupestris [33]	0.33	8.1	111.1	39.88	20.22	3.3	0.34
		0.45	10.4	107.1	53.23	20.81	4.06	0.38
	Tipula obsolete [45]	0.019	13.7	—	35.92	2.59	10.45	—
		0.011	12.7	—	29.51	1.89	10.93	—
	Tipula paludosa [45]	0.034	16.2	—	45.29	3.75	11.59	—
		0.05	17.4	—	53.82	4.54	11.25	—
		0.043	17.2	—	53.59	3.94	11.04	—
		0.052	10.2	—	23.84	10.6	8.73	—
		0.042	10	—	24.21	8.53	8.26	—
		0.035	10.2	—	25.59	6.65	8.13	—
		0.029	9.7	—	22.46	6.4	8.38	—
Bee		0.041	9.9	—	23.17	8.72	8.46	—
	Episyrphus balteatus [45]	0.014	9	—	19.49	3.52	8.31	—
		0.027	9.3	—	20.47	6.54	8.45	—
		0.028	10	—	25.25	5.46	7.92	—
		0.014	7.7	—	14.2	4.9	8.35	—
		0.022	9.5	—	21.88	4.98	8.25	—
		0.025	9.5	—	21.46	5.8	8.41	—
	Eristalis tenax [63]	0.068	11.4	—	36.35	9.23	7.15	—
		0.11	11.1	—	33.35	16.5	7.39	—
		0.1	9.8	—	28.5	17.5	6.74	—
		0.097	9.5	—	27.14	17.6	6.65	—
	Apis mellifera [63]	0.078	9.3	—	25.78	16.6	6.71	—
		0.097	9.6	—	28.01	17	6.58	—
		0.087	9.4	—	26.82	15.9	6.59	—
	Psithyrus vestalis [63]	0.19	14.3	—	63.21	14.6	6.47	—
		0.16	13.8	—	57.02	13.5	6.68	—
	Bombus terrestris [63]	0.22	14.3	—	63.9	17.1	6.4	—
		0.23	14.2	—	57.78	22.6	6.98	—
	Bombus hortorum [63]	0.23	14.1	—	59.08	18.8	6.73	—
	Bombus agrorum [31]	0.17	11.4	—	40.05	21.3	6.49	—
		0.14	11.4	—	38.28	18.3	6.79	—
	Bombus lucorum [63]	0.23	14.1	—	58.22	19.5	6.83	—

Table 1: Continued.

Species		m (g)	R (mm)	f (Hz)	S (mm^2)	p_w (N/m^2)	AR	k
	German wasp [69]	0.24	16.2	—	66.5	17.68	7.89	—
	European hornet [69]	0.6	21.5	—	152	19.25	6.08	—
	European hoverfly [69]	0.13	12.68	—	41.3	15.31	7.78	—
	Honey bee [69]	0.1	9.95	—	29.9	15.98	6.62	—
	Red-tailed bumblebee [69]	0.5	16.5	—	82.5	29.4	6.6	—
	Buff-tailed bumblebee [69]	0.39	16	—	71	26.78	7.21	—
	Bumblebee [70]	0.18	13	150	53	16	6.6	0.41
Coleoptera (beetle)	*Tibicen linnei* [33]	1.83	23.51	42.54	361.2	12.41	3.06	0.5
		1.85	23.35	44.1	356.5	12.74	3.06	0.51
		1.89	24.35	42.3	377	12.3	3.15	0.51
		1.81	23.55	42.9	359.55	12.36	3.08	0.51
		1.75	23.35	40.5	355.58	12.05	3.07	0.48
		1.84	22.95	42.9	357.38	12.61	2.95	0.5
	Allomyrina dichotoma [33]	4.29	22.23	37.46	322.14	32.73	3.07	0.25
		4.3	22.2	37	320	32.96	3.08	0.25
		4.5	24	36.1	366.5	30.11	3.14	0.28
		3.79	21.6	35.7	300.7	30.91	3.1	0.24
		4.61	22.4	39.5	329	34.36	3.05	0.27
		4.24	20.95	39	294	35.31	2.99	0.25
	Ladybird [60]	0.034	11.2	54	36.12	4.67	6.95	0.23
	Coccinella 7-punctata [63]	0.036	11.7	—	38.18	4.61	7.17	—
		0.027	11	—	34.04	3.85	7.11	—
		0.024	10.3	—	30.27	3.84	7.01	—
		0.034	11.2	—	35.49	4.76	7.07	—
		0.031	10.8	—	32.95	4.57	7.08	—
	Coleoptera [63]	0.597	—	62	222.5	13.15	—	0.4
		0.142	—	80	66.5	10.46	—	0.31
		0.291	—	78	114.5	12.45	—	0.37
Odonata (dragonfly)	*Anax parthenope* Julius [69]	0.79	71.6	—	995	3.89	10.305	—
		0.79	74.7	—	1090	3.55	10.245	—
	Damselfly [70]	0.045	29.9	27.5	118	1.86	15.15	0.34
		0.046	29.7	31.3	121	1.85	14.55	0.39
		0.052	29.1	34.1	115	2.2	14.7	0.38
		0.042	29.2	33.1	121	1.74	14.1	0.43
	Sympetrum flaveolum [33]	0.37	21.8	34.8	415.6	2.2	2.28	1.05
		0.33	21.65	38.5	416.4	1.97	2.26	1.24
		0.37	20.6	37.9	387.4	2.31	2.2	1.07
		0.31	20.95	35.3	370.1	1.93	2.22	1.04
	Aeschna juncea [71]	0.75	47.4	—	386.4	4.15	11.63	—
		—	46	—	—	4.15	8.4	—
	Odonata [72]	0.092	23.5	41	193.5	2.33	5.71	0.58
		0.101	27	44	255	1.94	5.72	0.78
		0.137	27.9	41	272.5	2.46	5.71	0.67
		0.102	22.5	41	177	2.82	5.72	0.51
		0.077	22.2	41	172.5	2.19	5.71	0.56
		0.09	25.4	46	226	1.95	5.71	0.77
		0.091	25.4	41	226	1.97	5.71	0.68

Table 1: Continued.

Species		m (g)	R (mm)	f (Hz)	S (mm^2)	p_w (N/m^2)	AR	k
	Battus polydamas [60]	0.45	53	12.4	1682.04	1.33	3.34	0.69
	Papilio thoas [29]	0.42	58.4	9.5	1937.82	1.07	3.52	0.63
	Parides childrenae [29]	0.37	46.1	12	1101.15	1.66	3.86	0.48
	Aphrissa boisduvalii [29]	0.14	32.5	13.7	1010.77	0.67	2.09	0.82
	Itaballia demophile [29]	0.089	28.4	11.7	653.09	0.66	2.47	0.57
	Archaeoprepona demophon [29]	1.06	60.4	8.9	2634.05	1.97	2.77	0.51
	Myscelia cyaniris [29]	0.091	31.6	9.1	715.82	0.62	2.79	0.48
	Pyrrhogyra naearea [29]	0.11	30.6	10.7	796.9	0.69	2.35	0.57
	Siproeta stelenes [29]	0.24	40.9	10.7	1203.46	0.98	2.78	0.58
	Dryas iulia [29]	0.18	44.1	13.9	764.17	1.12	5.09	0.55
	Janatella leucodesma [29]	0.024	18.1	13.3	246.32	0.48	2.66	0.47
	Morpho amathonte [29]	0.33	70.3	6.4	3594.25	0.45	2.75	0.89
	Morpho peleides [29]	0.36	60.5	6.9	2815.58	0.62	2.6	0.72
	Caligo illioneus [29]	1.04	74.3	9.6	4907.1	1.05	2.25	1.02
	Pierella luna [29]	0.077	35.1	13.7	772.42	0.49	3.19	0.84
	Ochlodes [33]	0.13	9.87	56.97	112.25	2.94	1.74	0.79
Butterfly		0.037	12.1	12.8	203.75	0.4	1.44	0.6
		0.039	12.1	9.9	229.35	0.42	1.28	0.51
	Pieris rapae [33]	0.042	11.4	12.7	225.35	0.46	1.15	0.62
		0.03	12.8	11.7	219	0.34	1.50	0.65
		0.05	12.3	13.1	253	0.49	1.20	0.66
		0.04	11.94	12.04	231.09	0.42	1.23	0.61
		0.06	7.35	43.5	60	2.43	1.80	0.47
		0.095	8.4	44.8	84	2.77	1.68	0.54
	Plusia gamma [33]	0.095	8.25	50.8	83.2	2.8	1.64	0.61
		0.065	8	47.6	72.85	2.2	1.76	0.6
		0.079	8	46.68	75.015	2.55	1.71	0.55
		0.13	9.55	56.6	110.95	2.78	1.64	0.77
	Ochlodes [33]	0.15	10.15	57.7	115	3.15	1.79	0.76
		0.13	9.9	56.6	110.8	2.89	1.77	0.77
	Scarce swallowtail [73]	0.38	36.99	—	1800	0.82	1.52	—
	Large white [73]	0.15	31.01	—	920	0.68	2.09	—
	Small heath [73]	0.05	15.99	—	240	0.94	2.13	—
		1.12	45.6	26.1	—	—	—	—
		1.83	43.5	25.9	—	—	—	—
	[12]	1.58	48.5	26.1	891	8.93	5.28	0.41
		1.65	51.9	26.3	953.5	8.53	5.65	0.43
		2	52.1	25.4	983.5	10.33	5.52	0.39
		1.41	49.7	28	994	6.95	4.97	0.52
	[74]	1.51	53.1	29	1067.3	6.93	5.28	0.56
Hawkmoth		1.29	51.6	31	1021.7	6.19	5.21	0.62
		1.47	50.8	27	909.3	7.92	5.68	0.45
	Emmelina monodactylus [45]	0.0084	11.1	—	42.56	0.97	5.79	—
		1.32	51.8	—	981.1	6.6	5.47	—
	Manduca sexta [45]	1.58	48.7	—	817.8	9.5	5.8	—
		1.39	46	—	759.8	8.96	5.57	—
		1.34	51.8	—	918.9	7.17	5.84	—
	[73]	1.69	48.51	—	900	9.2	5.23	—

Table 1: Continued.

Species		m (g)	R (mm)	f (Hz)	S (mm^2)	p_w (N/m^2)	AR	k
	[75]	1.67	49	25	891	9	5.3	0.38
	Giant peacock moth [73]	2.19	74.5	—	6000	1.54	1.85	—
	Death's-head hawkmoth [73]	1.67	51.02	—	1025	7.65	5.08	—
	Hummingbird hawkmoth [73]	0.29	21.3	—	189.5	7.29	4.79	—
	Soricina [76]	10.1	115	—	4266	11.3	6.2	—
		9.5	115	—	4266	10.8	6.2	—
	Yerbabuenae [76]	21.6	167.5	—	7903	13.4	7.1	—
		23.6	161.5	—	7671.25	15.1	6.8	—
	Glossophaga soricina [77]	11	119.72	—	4550	11.9	6.3	—
	Glossophaga soricina [78]	10.5	120.96	—	4645	11.2	6.3	—
	Leptonycteris yerbabuenae [79]	22.6	164.8	—	7760	14.2	7	—
	Cynopterus brachyotis [79]	30.7	197.55	—	11,650	13.14	6.7	—
	Pelcotus auritus [79]	9	134.69	—	6150	7.18	5.9	—
	Rousettus aegyptiacus [79]	118.3	276.42	—	28,300	20.5	5.4	—
		118.3	230.5	—	19,950	29.1	5.34	—
	Tadarida brasiliensis [79]	11.8	131.04	—	3504	16.5	9.8	—
	Chalinolobus gouldii [80]	13.4	173.06	9.04	8940	7.35	6.7	0.49
	Chalinolobus morio [80]	7	144.01	10.91	6755	5.08	6.14	0.62
	Chalinolobus nigrogriseus [81]	6.5	139.05	11.27	6090	5.24	6.35	0.6
	Hipposideros ater [32]	4.4	124.46	10.91	5305	4.07	5.84	0.61
	Macroderma gigas [32]	130	379.56	6.96	47,390	13.44	6.08	0.64
	Miniopterus schreibersii [32]	10.1	170.42	9.1	8370	5.91	6.94	0.53
	Mormopterus planiceps [80]	8.6	131.84	9.34	4795	8.69	7.25	0.34
	Nyctophilus arnhemensis [81]	7.1	150.71	11.43	7805	4.46	5.82	0.74
	Nyctophilus geoffroyi [32]	5.7	131.73	10.94	6110	4.74	5.68	0.62
Bats	*Nyctophilus gouldi* [82]	10	152.43	10.4	7985	6.14	5.82	0.58
	Nyctophilus timoriensis [80]	11	161.01	10.56	8670	6.22	5.98	0.61
	[32]	14.2	174.81	11.08	10,135	6.88	6.03	0.66
	Pteropus poliocephalus [32]	700	668.83	3.4	129,100	26.59	6.93	0.37
	Pteropus scapulatus [32]	412	552.87	4.15	82,500	24.5	7.41	0.37
	Rhinonycteris aurantius [32]	8.6	153.94	9.76	7535	5.6	6.29	0.56
	Saccolaimus flaviventris [83]	46.2	287.49	8.36	19,725	11.49	8.38	0.54
	Scotorepens balstoni [80]	8	133.09	11.31	5650	6.95	6.27	0.5
	Scotorepens greyii [81]	7	125.02	11.59	5050	6.8	6.19	0.49
	Tadarida australis [80]	35.3	231.28	8.19	12,920	13.4	8.28	0.39
	Taphozous georgianus [81]	28.1	233.22	8	14,055	9.81	7.74	0.47
	Taphozous hilli [32]	24.1	230.83	7.47	13,680	8.64	7.79	0.46
	Vespadelus finlaysoni [83]	5.6	127.5	10.68	5210	5.27	6.24	0.52
	Vespadelus regulus [80]	4.7	116.76	10.75	4455	5.17	6.12	0.49
	Egyptian fruit bat [84]	104	265	—	23,250	22	6.04	—
	Minor epauletted fruit bat [84]	50.36	200	—	14,500	18	5.52	—
	Common pipistrelle [84]	5.3	104.5	—	3250	8	6.72	—
	Common noctule [84]	26.5	172	—	8050	16	7.35	—
	Northern bat [84]	9.9	138.5	—	5750	8.4	6.67	—
	Parti-coloured bat [84]	14.12	149	—	6100	11	7.28	—
	Brown long-eared bat [84]	9	135	—	6150	7.2	5.93	—
	Large-eared free-tailed bat [84]	35.58	224.5	—	10,850	16	9.29	—

Table 1: Continued.

Species		m (g)	R (mm)	f (Hz)	S (mm^2)	p_w (N/m^2)	AR	k
	Blue-throated [85]	8.4	85	23.3	1763	23.5	8.2	0.31
	Magnificent [85]	7.4	79	24	1486	24.7	8.4	0.29
	Black-chinned [85]	3	47	51.2	622.3	23.5	7.1	0.41
	Rufous [85]	3.3	42	51.7	476.8	33.6	7.4	0.3
	[86]	3.2	46.1	—	599.2	36.7	7.1	—
	[87]	4.24	45	53.25	494	42.11	8.2	0.28
		4.24	48	49.1	584	35.61	7.89	0.31
		4.1	51	47.3	668.5	30.08	7.78	0.35
	Anna (male) [88]	4.54	52	42.57	662.5	33.6	8.16	0.29
		4.52	54.5	45.9	714	31.02	8.32	0.34
	[89]	5.6	50	—	588.2	—	8.5	—
		5	50	—	543.5	—	9.2	—
		4.7	59	—	838.8	—	8.3	—
Hummingbirds	Broad-tailed [87]	4.22	55	41.32	780.5	26.52	7.75	0.35
		3.46	54	36.38	736.5	23.05	7.92	0.32
		3.66	55	38.71	748	24.01	8.09	0.34
		5.16	57	39.25	799.5	31.67	8.13	0.31
		3.6	52	39.53	680.5	25.96	7.95	0.31
		3.61	56	37.17	817.5	21.66	7.76	0.35
		3.93	55	38.1	860.5	22.4	7.03	0.37
		4.1	57	37.94	837.5	24.02	7.76	0.35
	Ruby-throated (male) [90]	3.58	41	—	460	38.4	7.34	—
		3.67	41	—	485	37.3	6.96	—
		4.01	40	—	445	44.1	7.17	—
		4.16	43	—	455	44.9	8.13	—
	Ruby-throated (female) [90]	4.36	49	—	635	33.6	7.55	—
		4.36	48	—	640	33.3	7.18	—
		4.18	49	—	600	34.2	8	—
	Amazilia fimbriata [91]	5.1	58.5	35	850	29.4	8.05	0.29
	Aglaiocercus kingi smaragdinus [92]	4.65	61.2	21.7	988.9	23.34	7.58	0.22
	Chrysuroniaoerumejosephine [92]	4.6	54.1	32.8	748	30.35	7.82	0.25
	Lophomis delattrei [93]	2.79	40.3	50.7	394.8	34.5	8.23	0.27
	Phaethornis ruber [93]	2.64	40.7	40	484	27.2	6.83	0.26
	Giant hummingbird (male) [93]	22.6	143	13	4508.4	24	9.1	0.27
	(female)	19.6	139.7	13.9	4307.8	21.5	8.3	0.3
	Hypoleuca [76]	14.8	117.63	—	5293.43	13.7	5.2	—
		14.1	116.31	—	5234.09	13.2	5.3	—
		13.7	118.4	—	5327.78	12.6	5.2	—
	Atricapilla [76]	16.3	120.58	—	5546.53	14.4	5.2	—
	Adean condor [94]	11,700	1490	—	562,500	99.96	7.9	—
	Great bustard [94]	8950	1738	—	794,850	54.88	7.6	—
Birds	Wandering albatross [94]	8500	1703	—	310,300	134.26	18.7	—
	[94]	8877.6	—	—	310,000	140	—	—
	Griffon vulture [94]	7270	1278	—	527,000	67.62	6.2	—
	Brown pelican [94]	2650	1058	—	228,450	56.84	9.8	—
	Seagull [94]	1915	867.4	—	136,800	68.6	11	—
	White-fronted goose [94]	1715	703.5	—	91,650	91.14	10.8	—
	American black vulture [94]	1702	705	—	150,600	54.88	6.6	—

Table 1: Continued.

Species		m (g)	R (mm)	f (Hz)	S (mm^2)	p_w (N/m^2)	AR	k
	Pheasant [94]	1660	428.4	—	79,800	101.92	4.6	—
	Serpent eagle [94]	1655	909.7	—	206,900	39.2	8	—
	Frigate bird [94]	1620	1010	—	162,000	49	12.6	—
	Velvet scoter [94]	1578	484.6	—	50,500	152.88	9.3	—
	Black-throated loon [94]	1495	599	—	59,800	122.5	12	—
	Herring gull [94]	1189	728.5	—	106,150	54.88	10	—
	Mallard [94]	1100	446.7	—	46,400	117.6	8.6	—
	Red kite [94]	927	807.4	—	144,850	31.36	9	—
	Peregrine falcon [94]	712	505	—	57,300	60.76	8.9	—
	Carrion crow [94]	470	451.3	—	52,900	43.12	7.7	—
	Pigeon [94]	330	316.2	—	31,750	50.96	6.3	—
	Jackdaw [94]	253	353.4	—	33,300	37.24	7.5	—
	Long-eared owl [94]	247	471.2	—	54,150	22.54	8.2	—
	Kestrel [94]	245	367.1	—	35,000	34.3	7.7	—
	Montagu's harrier [94]	237	553.1	—	65,100	17.64	9.4	—
	Gray plover [94]	216	327.7	—	20,650	50.96	10.4	—
	Magpie[94]	214	297.8	—	32,250	32.34	5.5	—
	Little grebe [94]	180	220	—	11,800	74.48	8.2	—
	Merlin falcon [94]	173	303.7	—	20,500	41.16	9	—
	House sparrow [94]	30	123.1	—	5050	29.4	6	—
	Swift [94]	17	210.2	—	5200	16	17	—
	House martin [94]	14	147	—	4650	15.68	9.3	—
	Pied flycatcher [94]	12	116.5	—	4600	12.74	5.9	—
	Citril finch [94]	12	122.4	—	3700	15.68	8.1	—
	Stone chat[94]	12	108.4	—	3850	14.7	6.1	—
	Wren [94]	10	88.1	—	2250	23.52	6.9	—
	Gold crest [94]	4	71	—	1600	11.76	6.3	—
	Common tern [35]	117.3	—	—	25,000	23	—	—
	Dove prion [35]	173.5	—	—	23,000	37	—	—
	Black-head gull [35]	234.7	—	—	37,500	31	—	—
	Black skimmer [35]	306.1	—	—	44,000	34	—	—
	Common gull [35]	374.5	—	—	57,500	32	—	—
	Kittiwake [35]	398	—	—	50,500	39	—	—
	Royal tern [35]	479.6	—	—	54,000	44	—	—
	Fulmar [35]	836.7	—	—	62,000	66	—	—
	Herring gull [35]	959.2	—	—	90,500	52	—	—
	Great skua [35]	1377.6	—	—	107,000	63	—	—
	Great black-backed gull [35]	1959.2	—	—	136,000	71	—	—
	Sooty albatross [35]	2857.1	—	—	170,000	82	—	—
	Black-browed albatross [35]	3877.6	—		180,000	106	—	—

2.2. Wing Loading. Wing loading is an important parameter on the flight mechanism of flyers, which is defined as the weight of flyer divided by the total wing surface area and is expressed as follows:

$$p_w = \frac{mg}{A} \sim V_t^2 \sim l \sim m^{1/3}, \quad (5)$$

where p_w is wing loading (N/m^2).

Wing loading varies with the size and is proportional to the third root of the body mass and as a result inclining to be larger in larger animals and artificial flyers. Also, it has an equivalent unit of pressure. Therefore, it also presents the pressure force over the wing and is proportional to the square of the flight speed, which indicates that flyers with low wing loadings are able to fly in low speed. Meanwhile, (5) indicates that flyers with larger weight have larger wing loading and have to fly fast. Additionally, manoeuvrability

depends on wing loading, because it depends on the minimum radius of turn which is proportional to the body mass [37, 38]. In other words, manoeuvrability rises with wing loading decrease. Therefore, we could see that aircraft utilized in aerobatics has small wide wings with low wing loading.

2.3. Aspect Ratio. Aspect ratio is a parameter of the wing performance of flyers and a measure of the wing shape (wing slenderness along the spanwise). It is defined as the square of the wingspan over the wing pair surface, which is presented as follows:

$$\mathrm{AR} = \frac{(2R)^2}{2S} = \frac{2R^2}{S} \sim \frac{l^2}{l^2} \sim m^0. \tag{6}$$

It can be rewritten as

$$\mathrm{AR} = \frac{2R^2}{S} \approx \frac{2R^2}{(mg/2p_{\mathrm{w}})} \approx \left(\frac{4R^2}{mg}\right) p_{\mathrm{w}}. \tag{7}$$

From (6), it is observed that the aspect ratio does not vary with body mass, a dimensionless number. In (7), it presents that the aspect ratio can indicate the flight characteristics of flapping animals. The aspect ratio in hummingbirds is almost independent on size, whereas for other species the aspect ratio increases slightly with size. Details are available in [39].

In general, flyers with small aspect ratio have high agility as well as maneuverability, whereas a high aspect ratio wing contributes to a low induced drag, which facilitates a gliding and slow flapping flight. The induced drag caused by the lift tends to decrease with increasing aspect ratio. That is, induced drag is generally regarded to be inversely proportional to the aspect ratio. Therefore, the longer wing it is, the smaller induced drag is obtained. Impliedly, the glide ratio (the lift-to-drag ratio) rises with aspect ratio increase [39]. For instance, the aspect ratio of hummingbirds (approximately 6.5~9.5) is less than that of albatross (around 15), so albatrosses fly in gliding mode mostly, while hummingbirds are capable of hovering. Besides, increasing the aspect ratio will enhance the lift coefficient when the angle of attack is constant. Therefore, aerodynamic performance can be enhanced by increasing the aspect ratio. The higher the aspect ratio is, the longer and thinner the wing is. However, long wings are not always beneficial. It not only induces drag due to wingtip vortices but also is more vulnerable to break the wing. At the same time, the long wing might be negative to ground take-off.

Therefore, the different combinations of wing loading and aspect ratio allow a natural flyer to adopt particular flight pattern and foraging strategies [40]; see Figure 1. For instance, species of high wing loading and high aspect ratio, particular for short wing, usually fly fast and considerable inexpensive. Therefore, commuting and migrating species are usually adapted to such flight mode like swans, geese, and loons [41]. By contrast, flyers with low wing loading and low aspect ratio usually have a broad slotted wingtip since such kind of wingtip can act to delay stall and decline induced drag, avoiding too large wingtip vortices and rises to lift [42]. Otherwise, a smaller aspect ratio leads to high induced drag. Then, flying species with a high wing loading and low aspect ratio require very high energy cost such as gallinaceous, so they spend more time on the ground. Such kinds of animals have almost lost their flight capability such as penguins [43] (Penguin's wings might evolve into fins for swimming so as to adapt environmental conditions.) However, flyers that have low wing loading (large wing area) and high aspect ratio, particularly for flyers with small weight and long wing, fly slowly and inexpensively such as swallows and swifts. Certain natural flyers like bees, hummingbirds, and certain bats fly at unsteady flow environment and have a medium aspect ratio and wing loading. They are adapted to flight in hovering and foraging fly continuously in open spaces. Figure 1 (left) shows the aspect ratio plotted against wing loading for various natural flyers. From Figure 1 (right), we found that the butterfly has lower wing loading and aspect ratio than that of other species. In modern natural flyers, the aspect ratio ranges from 1.15 in some butterfly (*Pieris rapae*) to 18 (or higher) in wandering albatross. Besides, certain modern flyers have a similar combination of aspect ratio and wing loading, similarly to natural flyers. For instance, the space shuttle has a similar aspect ratio of butterflies with low wing loading. Boeings have a similar aspect ratio as hummingbirds.

Since wing loading and aspect ratio are widely applied to quantify the size and shape in aircraft engineering and studies of animal flight, here, the p_{w} – AR ratio is proposed as the ratio of wing loading to aspect ratio, and it is assumed $A \approx 2S$ in $(\mathrm{N/m^2})$

$$\begin{aligned} &p_{\mathrm{w}} - \mathrm{AR\ ratio},\\ &\frac{p_{\mathrm{w}}}{\mathrm{AR}} = \frac{mg/A}{2R^2/S} \approx \frac{mg}{2S} \bullet \frac{S}{2R^2} = \frac{mg}{4R^2}, \end{aligned} \tag{8}$$

It is observed that the p_{w} – AR ratio has the same physical unit of wing loading, so the p_{w} – AR ratio may have the same physical meaning of wing loading. The p_{w} – AR ratio presents the combination of wing loading and aspect ratio to evaluate the wing performances, which may be an evaluated performance index. Therefore, it may also be applied to assess the wing performances.

2.4. Flapping Wing Lift Production. To roughly estimate the effect of wing geometry parameters on the average lift force, a classical steady flow theory is employed when using cycle averaged quantities. The average lift force can be approximately presented as

$$\bar{F}_{\mathrm{L}} = \frac{1}{2}\rho \bar{C}_{\mathrm{L}}(2S)\bar{U}_{\mathrm{CP}}^2 = \rho \bar{C}_{\mathrm{L}} S \bar{U}_{\mathrm{CP}}^2. \tag{9}$$

It can be rewritten as

$$\frac{\bar{F}_{\mathrm{L}}}{S} = \rho \bar{C}_{\mathrm{L}} \bar{U}_{\mathrm{CP}}^2. \tag{10}$$

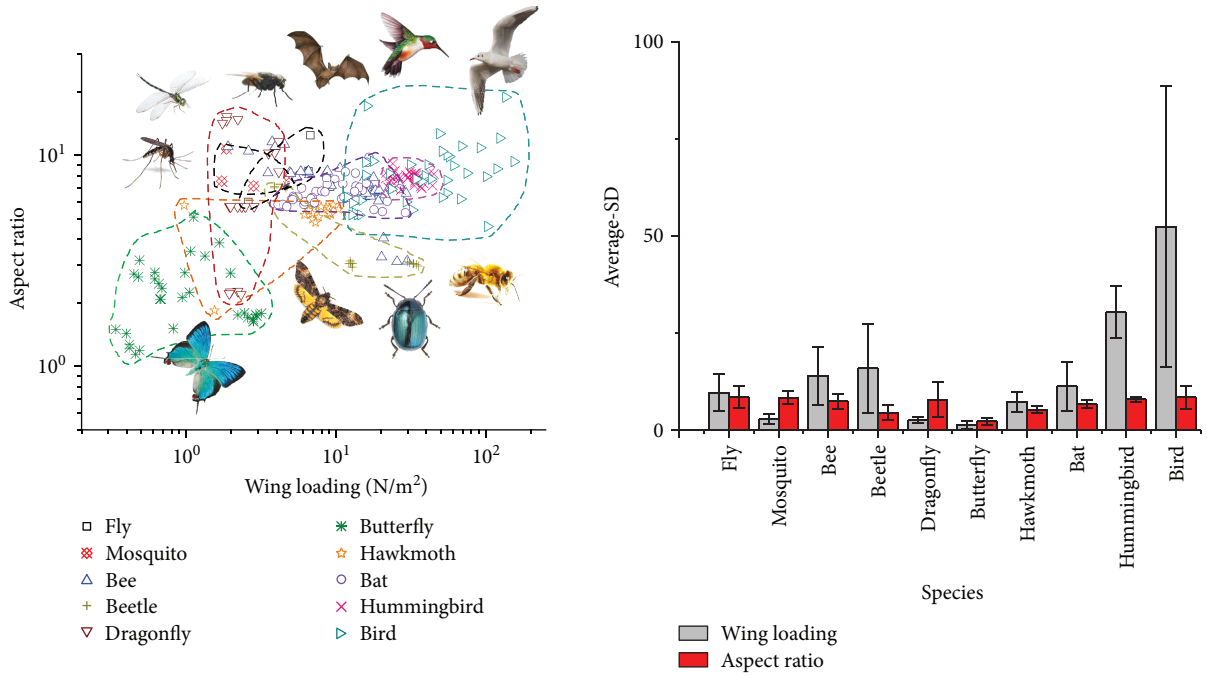

FIGURE 1: Aspect ratio vs. wing loading in natural flyers (left), and average value with standard deviation (SD) of wing loading and aspect ratio (right).

Therefore,

$$\overline{U}_{\mathrm{CP}} \sim \left(\frac{\bar{F}_{\mathrm{L}}}{S}\right)^{1/2} \sim (l)^{1/2} \sim (m)^{1/6}, \tag{11}$$

where $\overline{U}_{\mathrm{CP}}$ is the average velocity at pressure centre, which can be expressed as $\bar{U}_{\mathrm{CP}} = \sqrt{(\bar{F}_{\mathrm{L}}/S)/\rho\bar{C}_{\mathrm{L}}^2}$ and $\bar{C}_{\mathrm{L}}$ is the average lift coefficient which depends on wing geometry and attack angle variation over one wingbeat under the assumption of quasi-steady [44].

Assuming a flat and rigid wing with length R, the spanwise location of the pressure centre is given by the nondimensional radius of the second moments of wing areas $\widehat{r_2}(S)$, which ranges between 0.5 and 0.6 in most insects [45]. For the homogeneous pressure distribution on the whole wing, the second moment of the wing area coincides with the centre of pressure. Moreover, Lua et al. proved that the velocity at the second moment of the wing area can be selected as the reference velocity for flapping wings [46]. For simplicity, we assume $R_{\mathrm{CP}} = R/2$. Then, the average velocity at the pressure centre can be presented as

$$\bar{U}_{\mathrm{CP}} = 2\phi f R_{\mathrm{CP}} = \phi f R, \tag{12}$$

$$f = \frac{\bar{U}_{\mathrm{CP}}}{\phi R} \sim \frac{(l)^{1/2}}{l} = (l)^{-1/2} \sim (m)^{-1/6}, \tag{13}$$

where f is a wing flapping frequency (Hz) and ϕ is the flapping amplitude angle (deg).

Based on a combination of (6), (9), and (12), the cycle mean lift force of a pair of flapping wings can be reorganized as

$$\bar{F}_{\mathrm{L}} = \frac{1}{2}\rho\bar{C}_{\mathrm{L}}\mathrm{AR}(S\phi f)^2. \tag{14}$$

In (14), the average lift force is altered approximately linearly with $\bar{C}_{\mathrm{L}}$ and AR, but quadratically with the wing surface, flapping amplitude, and flapping frequency.

From the lift coefficient perspective, (14) can be rewritten as

$$\bar{C}_{\mathrm{L}} = \frac{2\bar{F}_{\mathrm{L}}}{\rho\mathrm{AR}(S\phi f)^2}. \tag{15}$$

2.5. Wing Lumped Parameter. Equation (14) indicates the relation of average lift force with the four variables such as AR, wing surface, flapping amplitude, and flapping frequency. This equation can be used to assess and guide wing design [20] but is unable to estimate the relation of wingbeat frequency with the four parameters (AR, wing surface, body mass, and flapping amplitude angle) because they are independent. Therefore, studying the relation between flapping frequency and body morphology (i.e., total wing surface and body mass) is indispensable. Corben [31] exhibited the relationship between flapping frequency and total wing surface A and body weight based on the nondimensional analysis, which is expressed as

$$f = \frac{k}{A}\sqrt{\frac{mg}{\rho}} = \frac{k}{A}\left(\frac{g}{\rho}\right)^{1/2}\sqrt{m} = 2.86\frac{k}{A}\sqrt{m}, \quad (16)$$

where the dimension of 2.86 is $\sqrt{m^4/s^2kg}$.

Therefore, the wing lumped parameter k can be expressed as

$$k = \frac{fA}{2.86\sqrt{m}} \sim \frac{m^{-1/6}m^{2/3}}{m^{-1/2}} = m^0. \quad (17)$$

Combination of (15) and (16) and the assumption of $\bar{F}_{\mathrm{L}} = mg$ in relation to the wing lumped parameter with mean lift coefficient and AR can be presented as

$$k = \frac{2\sqrt{2}}{\bar{C}_{\mathrm{L}}\varnothing\sqrt{\mathrm{AR}}} = \frac{2\sqrt{s}}{\bar{C}_L\varnothing R}. \quad (18)$$

The lumped parameter is also a dimensionless number. From (17), it is clearly seen that it does not vary with the body mass. As is shown in (18), the lumped parameter is inversely proportional to the average lift coefficient, which indicates that the larger the lumped parameter is, the less lift is produced at a constant angle attack. Additionally, the larger the lumped parameter is, the shorter and rounded the wing is. This is because the lumped parameter is also inversely proportional to the aspect ratio. Therefore, the lumped parameter may also be interpreted as a measure of aerodynamic efficiency, and the lumped parameter k may be used to supervise wing design.

The power functions of wing parameters and mass are summarized in Table 2 based on geometric similarity. We can see that the aspect ratio (AR) and the lump parameter (k) are independent on the mass, and the flapping frequency and wing loading are proportional to $m^{1/6}$ and $m^{1/3}$, respectively. Table 2 only shows the mathematical correlation while having no physical meaning.

3. Scaling Law, Results, and Discussion

In this section, the scaling laws induced from the regression analysis of species (insects, bats, hummingbirds, and other birds) are established through statistical analysis. The relation between weight and parameters of aerodynamic performance can be determined so that the relationship of different parameters, such as wing surface, wing length, flapping frequency, AR, lumped parameter, wing loading, and body mass, with aerodynamic performance can be predicted to MAV design. In other words, this concept provides rules to design and compare flying objects of different sizes and weight in different orders of magnitudes.

Many scholars conducted some similar studies, but no comprehensive and relevant works were done. Greenewalt [47] presented the earliest correlations linked with wingspan, wing surface, and mass among different bird species; however, the wing loadings were not provided. Likewise, a similar correlation on wingspan against mass and flapping frequency against mass was studied by Norberg [48]. Pennycuick [49] showed the database by fitting the date for different species of birds and bats and then studied the correlation among flapping frequency, body mass, and wing area. However, no comprehensive studies were conducted especially for the aspect ratio and lumped parameter. Therefore, this section examines the flow regime effects on body mass, flapping frequency, wing surface, wing loading, AR, and lumped parameter.

3.1. Wing Surface, Flapping Frequency, and Wing Length. The initial study objective is to assess the effect of wing surface, flapping frequency, and wing length. Wing geometries are varied during flapping. That is, the projected wing area and length are changed when flapping [36], which directly impacts on the lift or drag. To keep balance, the airfoil shape and posture of the body are also varied. To find the relation of wing surface and flapping frequency as a function of body mass and wing length, various species and data are surveyed. A summarized plot of the relation among wing surface, mass, and wing length is firstly presented in Figure 2. The optimal fitting of the wing surface is also provided in red color. From the figure, it is clearly seen that the data are highly intensive with an excellent general trend. In other words, the wing surface is proportional to both mass and wing length in a log–log domain. In Figure 2, the mass of flyers ranges from 0.7 mg to 3.8 kg. The rudimentary analysis shows that natural flyers in general track follow the rules. The relation between wing single surface and the mass of natural flyers can be expressed as follows:

$$\mathrm{S} = 430.29m^{0.77}. \quad (19)$$

The relation between single wing surface and wing length is shown in Figure 2 (right); the equation can be written as

$$\mathrm{S} = 0.81R^{1.81}. \quad (20)$$

Figure 3 shows the flapping frequency related to body mass and wing length, respectively. Figure 3 (left) reveals the relation between flapping frequency and mass. The general trend is presented with an inverse proportion in the log–log domain, which can be roughly expressed as

$$f = 40.63m^{-0.29}. \quad (21)$$

The relation between flapping frequency and wing length is shown in Figure 3 (right), and the fitted equation can be still roughly written as

$$f = 740.31R^{-0.82}. \quad (22)$$

As shown in Figure 3, high frequency is an option of insects or small birds such as hummingbirds, but not of larger birds, because their bones cannot bear the stress caused by a heavier inertial load. Smaller birds, bats, and insects are likely to choose higher frequency because of the decreased inertial loading within the limited breaking stress of their hollow bones. Also, the data in Figure 3 is slightly scattered; this might result from their distinct flight pattern of different species. From (19) to (22), we can see that the wing surface

Table 2: Power function of wing parameters against body mass. The exponent of correlations is for $(\text{mass})^{\text{exponent}}$.

Wing parameters	R	$\bar{c}$	S	p_w	AR	k	$\bar{U}_{CP}$	f
Dimensions	(mm)	(mm)	(mm^2)	(N/m^2)	—	—	(m/s)	Hz
Exponent of correlation	$m^{1/3}$	$m^{1/3}$	$m^{2/3}$	$m^{1/3}$	m^0	m^0	$m^{1/6}$	$m^{1/6}$

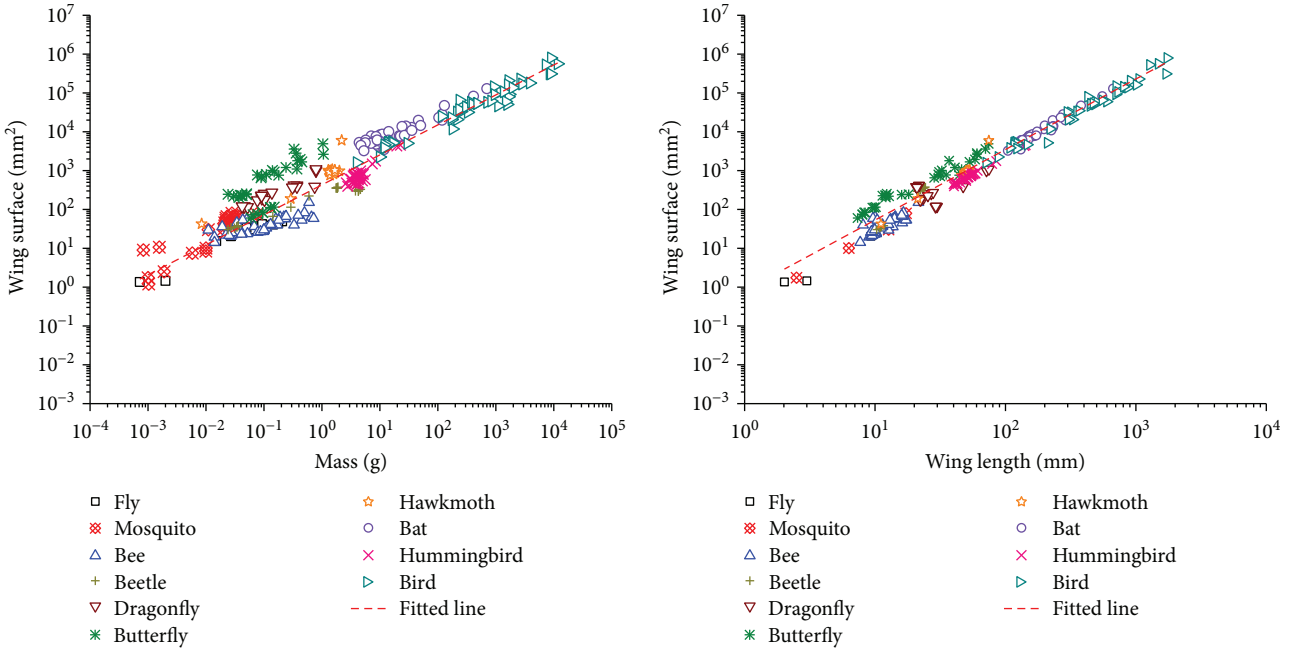

Figure 2: The relation of wing surface vs. mass (left), and wing surface vs. wing length (right).

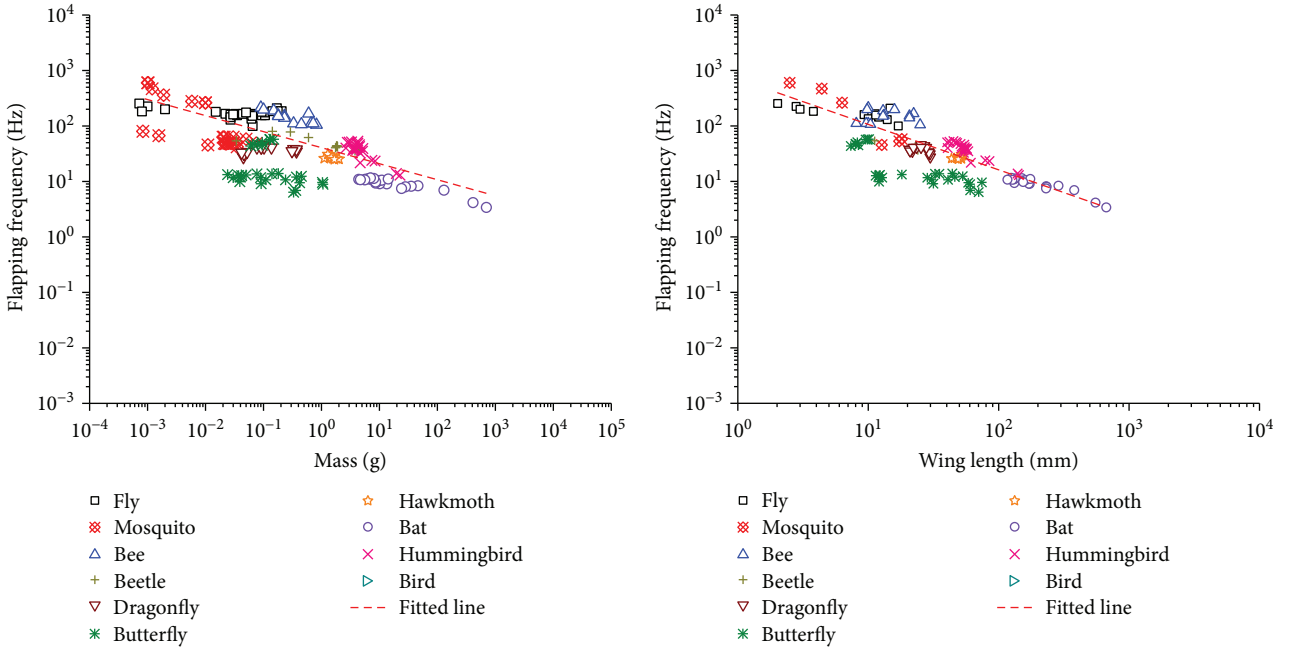

Figure 3: The relation of flapping frequency vs. mass (left), and flapping frequency vs. wing length (right).

increases with their body mass and the wing length increases, while the flapping frequency decreases with their body mass and the wing length increases.

The relationship between wing length and body mass is shown in Figure 4. In this figure, it is observed that the data of natural flyers are intensive and track the following rule and the wing length is positively proportional to the body mass. The equation of the dashed line of all species is

$$R = 43.31m^{0.39}. \quad (23)$$

According to the preceding equation, the relationship among wing area, wing length, flapping frequency, and body mass are clearly and easily observed, although data in Figure 3 are not much intensive. Therefore, the conclusion from the above observations indicates that the general laws related to wing surface, wing length, flapping frequency, and body mass exist and can be applied to guide the wing design of flapping wing MAVs.

3.2. Wing Loading, Aspect Ratio, and Lumped Parameter. Wing loading is an important parameter when studying flight mechanisms in flyer science. Wing loading analyzes the opposing action of two category forces, such as gravitational and inertial forces, and the aerodynamic forces to generate lift and thrust. Wing loading p_w mainly represents the wing flapping effect of a flyer. The relation of wing loading with body mass and wing length is shown in Figure 5. Generally, the wing loading rises with the mass increase, which is the response to (5). This is really the case for certain species such as bat ($p_w \sim m^{0.29}$), whereas other species may not follow this rule such as hummingbirds ($p_w \sim m^{-0.16}$). A similar result was also presented in [43]. The data in Figure 5 are moderately scattered, which might be related with the aerodynamic and structural factors. For instance, birds use pectoral muscles to perform downstroke motions and supracoracoideus muscles for upstroke motions [50], whereas insects or bats have different movements. Besides, it is clearly seen that the wing loading in butterfly is smaller than that of other species, which may be linked that they have a relatively larger wing surface. The data from other species are also mildly intensive (except butterfly). The slope of the interpolating straight line can be obtained, showing an acceptable performance. The equation of the straight line is

$$p_w = 10.85m^{0.25}. \quad (24)$$

The relation between wing loading and wing length is presented in Figure 5 (right), and the corresponding equation can be expressed as

$$p_w = 1.52R^{0.55}. \quad (25)$$

From (24) and (25), we also know that the wing loading rises with increasing their body mass and wing length.

Aspect ratio AR and the lumped parameter k are also essential parameters that are directly related to the wing shape, such as the wing length, and wing surface thereby affecting the aerodynamic performance. Aerodynamic performance

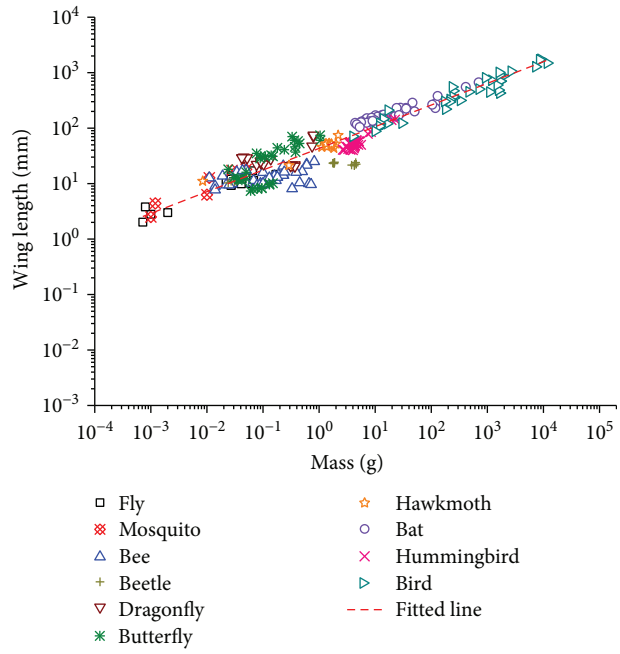

Figure 4: Relation of wing length vs. mass.

can be enhanced by making the wings longer and thinner. This is the reason why high performances of gliders have a nearly 20 aspect ratio, whereas aircrafts applied in aerobatics possess short broad wing for high manoeuvrability.

As previously mentioned, the aspect ratio is independent of size in geometric similarity analysis. However, the ratio for other species excluding hummingbirds rises slightly in size. Similarly, the lumped value is also constant based on (17). In this study, the average value of various species is considered and studied. From (18), it can be observed that the aspect ratio and lumped parameter are in inverse proportion, which indicates that the species with high aspect ratio have a lower lumped parameter. The relationship of AR and lumped parameter k with body mass and wing length are plotted in Figures 6–8. Figure 6 (left) shows AR against mass, whereas Figure 6 (right) indicates the relation of AR and wing length for various natural flyers. From Figure 6, it is found that the data of species except for butterfly is intensive and consistent around the average value. Nevertheless, both figures evidently show an obtained average aspect ratio which is approximately 7.16 for all species presented in this paper, except for butterflies. The performance of butterflies may be caused by unique wing structure, relative large wing surface, and flapping wing motion.

In Figure 7 (left), the relation of k and mass is shown, and in Figure 7 (right), the relation between k and wing length is also exhibited. All data is well distributed and close to the average value of 0.48, which indicates that lumped parameter k may constantly be free from the mass and wing length for natural flyers. Therefore, according to the lumped parameter k and (13) and (15), the relation of flapping frequency, wing total surface, and mass can be established. Furthermore, the relationship of wing single surface, lift coefficient, flapping

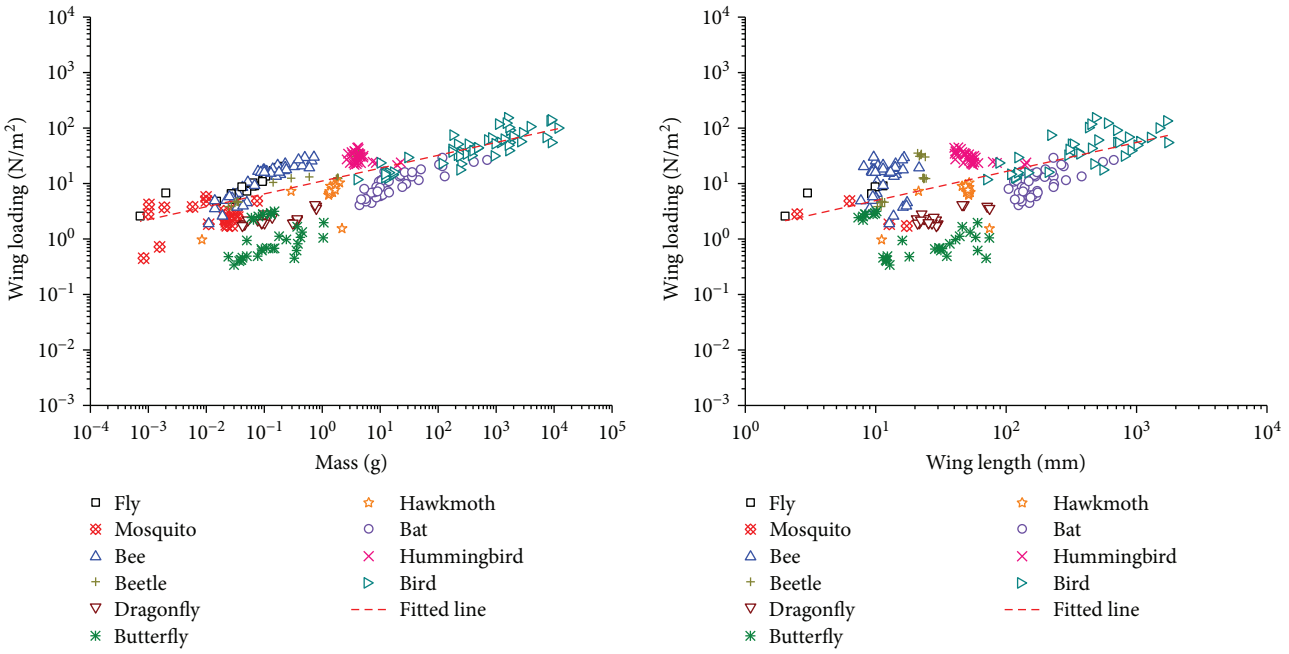

Figure 5: The relation of wing loading vs. mass (left), and wing loading vs. wing length (right).

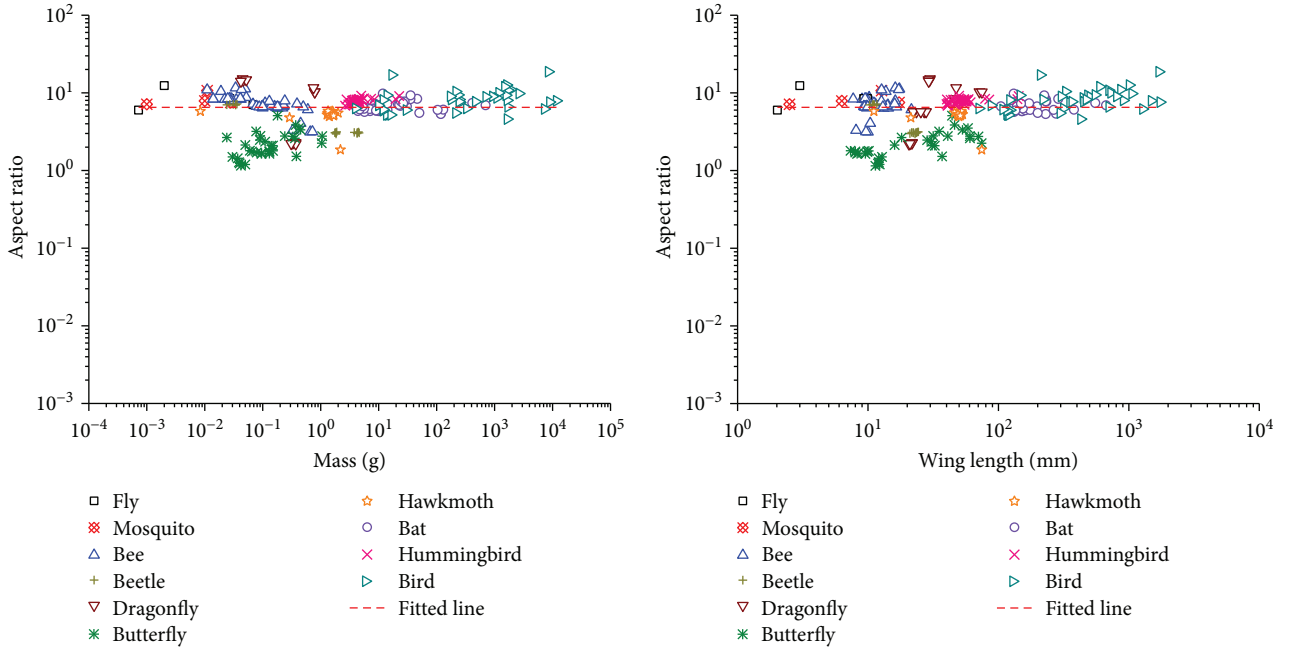

Figure 6: Relation of aspect ratio vs. mass (left), and aspect ratio vs. wing length (right).

amplitude, aspect ratio, and wing length can be roughly obtained as well.

In this section, a comprehensive study is performed regarding the aspects of wing length, wing surface, body mass, and flapping frequency, specifically for the aspect ratio and lumped parameter k of natural flyers, which is summarized in Table 3 for each species. The aspect ratio and lumped parameter for each species are presented in mean value with standard deviation. The data is of 0.01 precision. New findings are valuable and useful. The average aspect ratio in the natural flyer excluding butterflies is nearly 7.16, and the average lumped parameter in the natural flyers is approximately 0.48. The aspect ratio and lumped parameter corresponding to the species are presented in Figure 8. It is found that the butterfly has a low aspect ratio and high lumped value k. In short, the summarized relation presented in Table 3 provides a reference when designing flapping wing MAVs inspired by natural flyers.

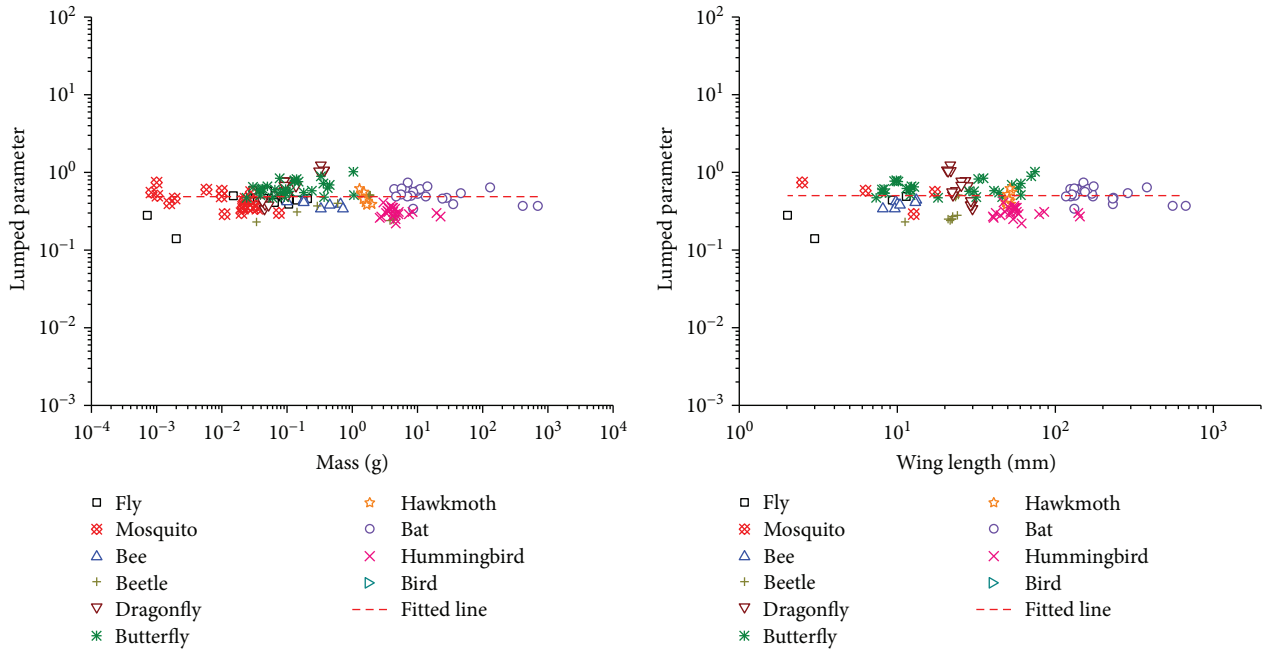

Figure 7: Relation of lumped parameter and mass (left), and lumped parameter vs. wing length (right)[1]. (1. The distribution of the data is lightly different in the two graphs because of absence of certain figures, which are indicated as "—" in Table 1.)

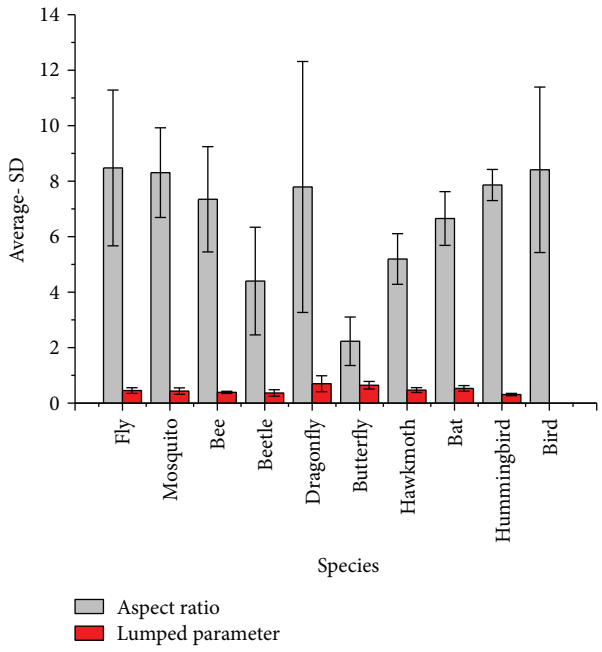

Figure 8: Lumped parameter and aspect ratio in natural species.

Due to the less survey numbers, the power functions of flapping frequency and lump parameter against body mass for bird are not given. Also, the butterfly has a lower aspect ratio and higher lumped value compared with other species, which is opposite to that of hummingbirds. Interestingly, the power function of wing loading for hummingbirds is entirely different from other species. Also, Table 3 only shows the mathematical relation while having no physical meaning.

3.3. Wing Design and Manufacture for Flapping Wing MAVs. Based on the study above, the relations among different parameters are presented and summarized in Table 3. In this section, the existing flapping wing MAVs are added for comparison. The morphological parameters of flapping wing MAVs are shown in Table 4. Here, the relation of wing surface and wing length against mass as well as lumped parameter against aspect ratio including flapping wing MAVs are separately discussed and studied as examples.

According to the relation between single wing surface, wing length, and the mass of natural flyers, it is observed that the size of MAVs obeys such rule; see in Figure 9. Currently, the existing flapping wing MAVs are nearly in the range of corresponding species, in which the size of KUBeetle is close to the size of giant hummingbird, whereas the size of Maryland-Hummingbird, DelFly-II, and TL-FlowerFly are in the scope of Bat. They are highlighted in black with dots. Figure 10 reveals the relation lumped parameter and aspect ratio in all flyers including natural and manufactured flyers. From Figure 10, we can observe that the lumped value k of Bee and Hummingbird is lower than the average value of natural species, which is marked in blue and pink shadows. The lumped value of DelFly-II is above the average value, and then that of Harvard-RoboBee and Maryland-Hummingbird is almost equal the mean value of k, whereas others are all less than the mean value of k. It indicates that the wing efficiency of DelFly-II might be not perfect, but acceptable, which can be evidenced as well in Figure 11. In Figure 11 (left), it is clearly seen that the wing loading of

Table 3: Power functions of wing dimensions and flight parameters vs. body mass.

	R (mm)	f (Hz)	S (mm^2)	p_w (N/m^2)	AR	k
All species	$43.31m^{0.39}$	$40.63\,m^{-0.29}$	$430.29m^{0.77}$	$10.85m^{0.25}$	7.16 ± 1.47	0.48 ± 0.13
Brachycera (fly)	$27.16m^{0.27}$	$140.83\,m^{-0.054}$	$93.06m^{0.39}$	$54.68m^{0.62}$	8.48 ± 2.81[a]	0.45 ± 0.10
Coleoptera (beetle)	$71.10m^{0.43}$	$14.12\,m^{-0.48}$	$459.17m^{0.61}$	$3.31m^{0.037}$	8.31 ± 1.62	0.44 ± 0.12
Nematocera (mosquito)	$17.38m^{0.14}$[b]	$99.02\,m^{-0.30}$	$97.90m^{0.39}$	$33.72m^{0.41}$	7.35 ± 1.90[c]	0.39 ± 0.04
Bee	$19.41m^{0.14}$	$48.46\,m^{-0.13}$	$230.68m^{0.33}$	$10.40m^{0.75}$	4.4 ± 1.94	0.37 ± 0.12[d]
Odonata (dragonfly)	$57.13m^{0.36}$	$40.93m^{0.036}$	$964.24m^{0.71}$	$3.56m^{0.23}$	7.79 ± 4.52	0.70 ± 0.29
Butterfly	$74.39m^{0.53}$	$19.16\,m^{-0.090}$	$3825.99m^{0.83}$	$1.60m^{0.095}$	2.23 ± 0.87	0.64 ± 0.14
Hawkmoth	$42.32m^{0.42}$	$29.34\,m^{-0.20}$	$56.94m^{5.71}$	$7.07m^{0.20}$	5.19 ± 0.91	0.47 ± 0.09[e]
Bats	$60.16m^{0.36}$	$15.59\,m^{-0.19}$	$862.71m^{0.76}$	$4.55m^{0.29}$	6.65 ± 0.97	0.53 ± 0.10
Hummingbird	$21.07m^{0.62}$	$88.25\,m^{-0.57}$	$133.42m^{1.15}$	$38.27\,m^{-0.16}$	7.86 ± 0.56	0.31 ± 0.04
Bird	$36.98m^{0.41}$	—	$349.11m^{0.80}$	$9.71m^{0.27}$	8.41 ± 2.98	—

The accuracy of average value of (a), (c), (d), (e), and formula (b) will be low due to the less survey numbers. The data in AR and k are displayed as mean ± SD.

Table 4: Parameters of existing flapping wing MAVs.

Species	m (g)	R (mm)	f (Hz)	S (mm^2)	p_w (N/m^2)	AR	∅ (deg)	k
ASL-Colibri [10]	22	90	22	1816	52.43	8.9	180	0.21
Nano hummingbird [8]	17.5	68	27.5	1768	49.5	5.2	180	0.26
Maryland hummingbird [9]	62.1	140	20	9232	33.4	4.2	120	0.52
KUBeetle [3]	21.4	70	25–35	1750	50.7	5.6	190	0.3
Harvard-RoboBee [2]	0.08	15	120	52	15.1	8.7	110	0.49
DelFly II [4]	17	140	13	11,195	3.72	3.5	44	0.78
TL-FlowerFly [5]	16.6	100	10	6100	6.67	3.3	90	0.33

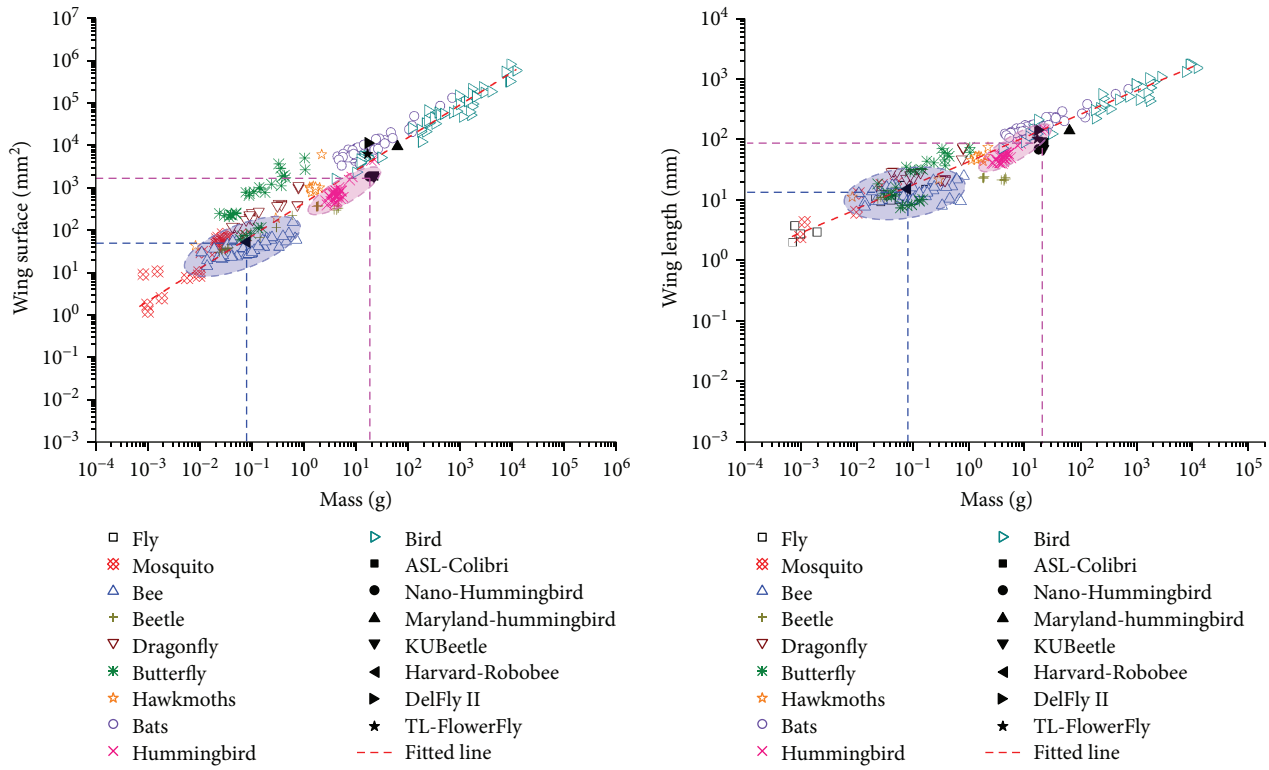

Figure 9: Relation wing surface, wing length vs. mass including the MAVs.

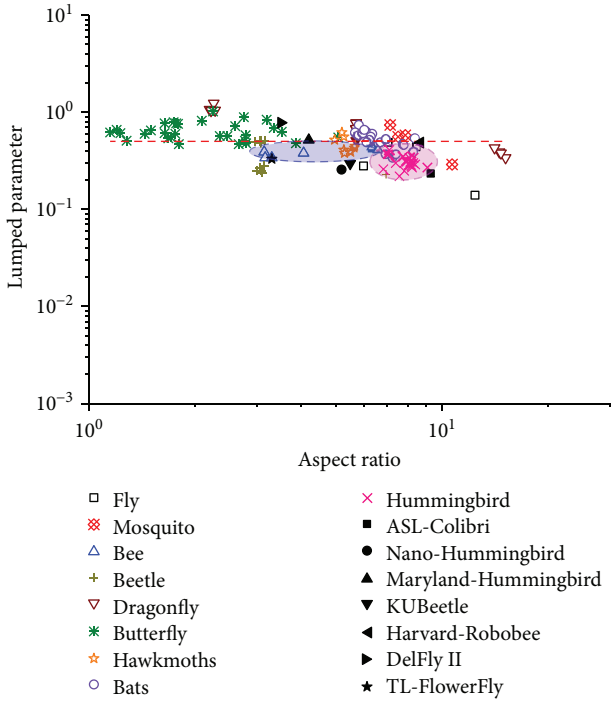

FIGURE 10: Relation lumped parameter vs. aspect ratio including the flapping wing MAVs.

ASL-Colibri, KUBeetle, and Nano Hummingbird are similar and larger than others, which means more lift can be produced per square meter. By contrast, the wing loading of Harvard-RoboBee is lower in the twin-wing flapping wing MAVs; thus, it means that it might cost more energy per unit force. Also, in X-wing flapping wing MAVs, the wing performance of TL-FlowerFly seems better than that of DelFly-II. In Figure 11 (right), the $p_w - AR$ ratio in Harvard-RoboBee is less than others, which reveals that it may not have an excellent wing performance. Also, it might be associated with the flexibility of the wing. Regarding Maryland-Hummingbird, the good performance is exhibited, although its wing loading is small.

The lift generation is linked not only to the wing performance, such as wing surface, frequency, and wing length, but also to other properties, such as wing materials, the position of a stiffener, flexural stiffness, and wingtip shape. For instance, a rounded wing for a given span generates an elliptic transverse lift distribution, which contributes to a minimum induced drag and a constant lift coefficient along the wingspan. And the tapered aft-swept tips produce less drag for a given lift and extract more energy from the vertical wake [51]. According to the study of Shyy et al. [52], overly flexible wings will result in inefficient aerodynamic performance. The lift is also affected by the wing fabrication process. Currently, many category wing shapes are designed using different materials, such as Nylon, Latex, PVC film, and Mylar. At hummingbird scale, many wings, such as those of Nano hummingbird [53] and ASL-Colibri [20], are made using the traditional simple method of cut-and-edge because it is simple and easily repeatable. In Nan et al.'s study [20], wings of ASL-Colibri are made of Mylar membrane (15 μm) and CFRP stiffeners (width = 1 mm; thickness = 0.12 mm) and are thus subjected to deformation when flapping. The principal steps of wing production shown in Figure 12 are similar to that of Nano hummingbird [53]. According to the flight demonstration of ASL-Colibri shown in Figure 13, the designed wing based on scale law in this paper is reasonable, and the lift test results are precise and repeatable (see details in [20]), thereby enabling a 17.2 g ASL-Colibri vehicle to fly.

At insect scale, the microelectromechanical systems (MEMS) are employed to construct wing design because these systems improve the quality of accuracy and repeatability, for example, in the case of the Harvard-RoboBee [54] and the KUBeetle [55]. Impliedly, to reduce the vehicle size, the miniaturization should be overcome since the traditional method does not offer adequate precision and repeatability [56]. Some wings are manufactured by CNC machines, such as DelFly II [4] and wings designed by Chang et al. [57]. Additional details of wing designs based on different materials and methods are summarized in Table 5.

4. Conclusions and Future Works

In this paper, the geometric similarity is first studied. The $p_w - AR$ ratio is then defined to estimate wing performance and aerodynamic performance. After that, the comprehensive scale laws are studied and achieved for natural flyers. Besides, the lumped parameter is first comprehensively studied. It is observed that the relationship between the aspect ratio and the lumped parameter is inversely proportion and the lumped parameter is independent to the body mass through geometric similarity analysis. Via statistical study among natural flyers, the lumped parameters are nearly constant from the body mass. The power functions of wing dimensions and flight parameters against the body mass are also summarized. These functions might vary on the number of natural flyers surveyed, but the achieved relationships indicate the universal tendencies, and it is verified that the performance of artificial wings in flapping wing MAVs follow these scaled rules. Therefore, the obtained scale laws are acceptable. Last, the wing manufacture of ASL-Colibri is interoperated as an example, and take-off demonstration of ASL-Colibri is also performed, which indicates that the designed wings based on the obtained scale law in this paper are acceptable. Moreover, artificial wings, including fabrication materials and methods, are summarized. Summarily, the current study will provide a useful dataset as a reference for future research. These results provide a simple but powerful guideline for biologists and engineers who are studying the morphology of natural flyers and designing flapping wing MAVs.

In our future work, we will focus on (1) the optimal design and advanced simulation on the flapping wing MAV via computational intelligence-assisted design (CIAD) [58] and (2) improvement of the MAV design by developing reliability indices for capturing the time-varying and nonlinear dynamical performance during experimental studies; (3) furthermore, we will look at the intelligent

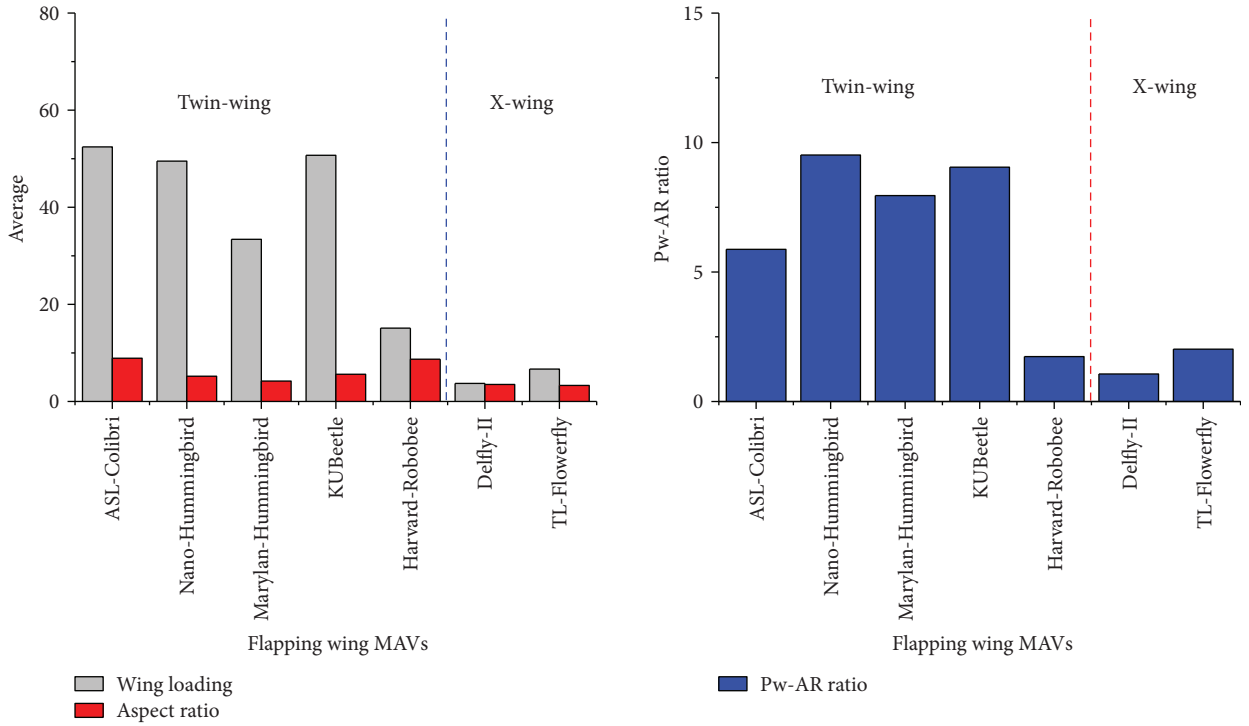

FIGURE 11: Wing loading and aspect ratio for flapping wing MAVs (left) and p_w – AR ratio (right).

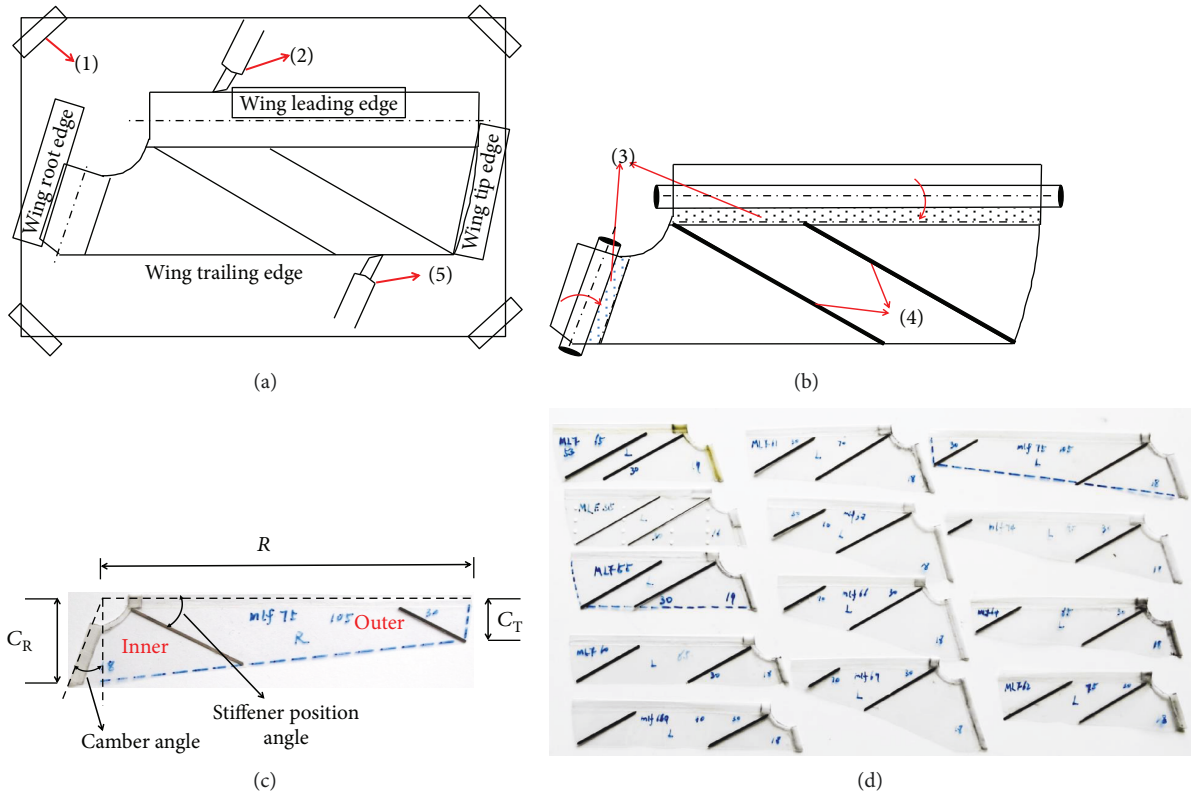

FIGURE 12: Principal steps of wing production and certain selected wings. (a)–(b): (1) mylar foil is taped on top of a printed template with desired wing geometry. (2) The contours of future wing sleeves are cut out. (3) Strips of Teflon are placed at the position of wing bars and fixed. Glue (Pattex contact glue diluted 1:1 with acetone) is applied, and the sleeves are completed by folding the foil around the Teflon strips. (4) Glue is applied at the position of stiffeners and the stiffeners are glued. (5) The rest of the wing is cut out, and the Teflon strips are removed. (c) Wing geometry: C_T wing tip chord and C_R wing root chord. (d) Certain selected wings [20].

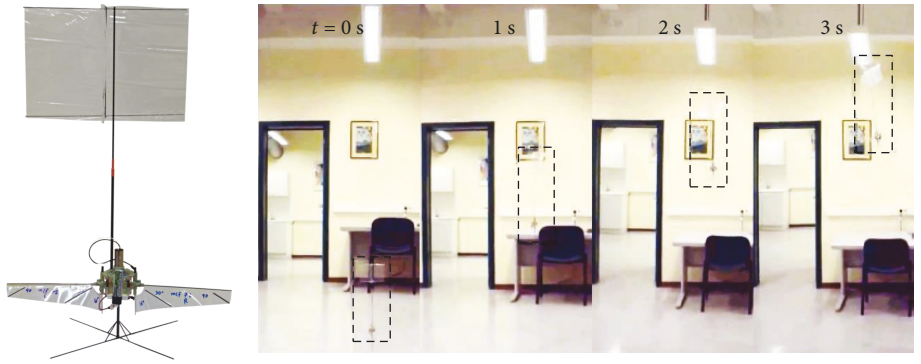

(a) (b)

Figure 13: Take-off demonstration with sail-like damper for passive stability: photo of the prototype vehicle used in the test (a) and take-off sequence (b). The full video recording is available online: https://youtu.be/oaFR815dtIo [20].

Table 5: Artificial wings, including fabrication materials and methods.

Authors	Model	Wing model (cm)	Fabrication method	Materials	
				Veins	Membrane
Bontemps et al. [95]	—	MEMS-based		SU-8	Parylene
Roll et al. [96]	—	Cut-and-glue		Carbon fiber	Mylar
Watman and Furukawa [97]	—	—		Carbon pultrusions	Mylar
Sahai et al. [98]	—	SCM		Titanium alloy with carbon fiber reinforcement	Ultra polyester film
Kim et al. [99]	—	Cut-and-glue		Graphite/epoxy composite	Flexible PVC
Campolo [100]	Dipteran	Chemical vapor deposition and molding		Carbon fiber	Cellulose acetate film
Wood [101]	Dipteran	SCM		Carbon fiber	Mylar
Nguyen et al. [102]	Insects	Cut-and-glue with paper mold		Carbon rods	Mylar
Lentink et al. [103]	Dragonfly	Cut-and-glue with paper mold		Carbon rods	Mylar
Meng et al. [104]	Hoverfly *Syrphidae*	MEMS-based		SU-8	Polyimide
Tanaka and wood [105]	Hovering Eristalis	Micro molding		Thermosetting resin	—
Ma et al. [106]	Hovering Eristalis	SCM		Carbon fiber	Mylar
Pornisin-Siriak et al. [107]	Bat	MEMS-based		Titanium alloy with carbon fiber reinforcement	Parylene
Ho et al. [50]	Cicada	MEMS-based		Titanium alloy with carbon fiber reinforcement	Parylene
Keennon et al. [8]	Hummingbird	—		Carbon fiber	—
Tanaka et al. [108]	Hummingbird	—		Carbon fiber-reinforced plastic	Parylene
Coleman et al. [9]	Hummingbird	Mold-glue		Carbon fiber	1/32 foam membrane
Nan et al. [20]	Hummingbird	Cut-and-glue		Carbon fiber	Mylar

control for the autonomous MAV using artificial intelligence algorithms via CIAD.

Nomenclature

A: Total surface, m^2
AR: Aspect ratio
$\bar{c}$: Mean wing chord, mm
C_L: Lift coefficient
$\bar{C}_L$: Mean lift coefficient
f: Wingbeat frequency, Hz
$\bar{F}_L$: Mean lift force, N
g: Gravitational acceleration, m/s^2
k: Wing lumped parameter
l: Characteristic length, m
m: Flyer mass, g

p_w: Wing loading, N/m^2
p_w – AR ratio: The ratio of wing loading to aspect ratio
R: Single wing length, mm
S: Single wing surface, mm^2
$\bar{U}_{CP}$: Average velocity at pressure centre, m/s
V: Volume, m^3
V_t: Forward flight velocity, m/s
W: Weight, N
ρ: Air density, kg/m^3
ϕ: Flapping amplitude angle, deg.

Data Availability

The data used to support the findings of this study are available from the corresponding author upon request.

Conflicts of Interest

The authors declare that they have no conflicts of interest.

Acknowledgments

The authors would like to acknowledge the partial supports provided by the National Natural Science Foundation of China (No. 51575090), the Artigent Young Talent Scholarship Award, and the Dean's Scholarships for International Academic Excellence, School of Engineering and Built Environment, Glasgow Caledonian University.

References

[1] X. Deng, L. Schenato, W. C. Wu, and S. S. Sastry, "Flapping flight for biomimetic robotic insects: part I-system modeling," *IEEE Transactions on Robotics*, vol. 22, no. 4, pp. 776–788, 2006.

[2] R. J. Wood, "The first takeoff of a biologically-inspired at-scale robotic insect," *IEEE Transactions on Robotics*, vol. 24, no. 2, pp. 341–347, 2008.

[3] H. V. Phan, T. Kang, and H. C. Park, "Design and stable flight of a 21 g insect-like tailless flapping wing micro air vehicle with angular rates feedback control," *Bioinspiration & Biomimetics*, vol. 12, no. 3, 2017.

[4] B. Bruggeman, *Improving Flight Performance of DelFly II in Hover by Improving Wing Design and Driving Mechanism*, Delft University of Technology M. Sc. thesis, 2010.

[5] Q. V. Nguygen, W. L. Chan, and M. Debiasi, "Performance tests of a hovering flapping wing micro air vehicle with double wing clap-and-fling mechanism," in *International Micro Air Vehicles Conference and Flight Competition*, pp. 1–8, Aachen, Germany, 2015.

[6] Festo Corporate, "Dragonfly," Festo Report, 2013.

[7] Festo Corporate, "Butterfly," Festo Report, 2015.

[8] M. Keennon, K. Klingebiel, and H. Won, "Development of the nano hummingbird: a tailless flapping wing micro air vehicle," in *50th AIAA Aerospace Sciences Meeting including the New Horizons Forum and Aerospace Exposition*, Nashville, Tennessee, January 2012.

[9] D. Coleman, M. Benedict, V. Hrishikeshavan, and I. Chopra, "Design, development and flight-testing of a robotic hummingbird," in *AHS 71st annual Forum*, pp. 1–18, Virginia Beach, Virgina, 2015.

[10] A. Roshanbin, H. Altartouri, M. Karásek, and A. Preumont, "Colibri: a hovering flapping twin-wing robot," *International Journal of Micro Air Vehicles*, vol. 9, no. 4, pp. 270–282, 2017.

[11] Festo Corporate, "Smartbird," Festo Report, 2011.

[12] A. P. Willmott and C. P. Ellington, "The mechanics of flight in the hawkmoth Manduca sexta. I. kinematics of hovering and forward flight," *Journal of Experimental Biology*, vol. 200, Part 21, pp. 2705–2722, 1997.

[13] S. A. Ansari, K. Knowles, and R. Zbikowski, "Insectlike flapping wings in the hover part II: effect of wing geometry," *Journal of Aircraft*, vol. 45, no. 6, pp. 1976–1990, 2008.

[14] N. Phillips, K. Knowles, and R. J. Bomphrey, "The effect of aspect ratio on the leading-edge vortex over an insect-like flapping wing," *Bioinspiration & Biomimetics*, vol. 10, no. 5, 2015.

[15] K. B. Lua, Y. J. Lee, T. T. Lim, and K. S. Yeo, "Aerodynamic effects of elevating motion on hovering rigid hawkmothlike wings," *AIAA Journal*, vol. 54, no. 8, pp. 2247–2264, 2016.

[16] A. Pelletier and T. J. Mueller, "Low Reynolds number aerodynamics of low-aspect-ratio, thin/flat/cambered-plate wings," *Journal of Aircraft*, vol. 37, no. 5, pp. 825–832, 2000.

[17] S. Deng, M. Percin, and B. van Oudheusden, "Experimental investigation of aerodynamics of flapping-wing micro-air-vehicle by force and flow-field measurements," *AIAA Journal*, vol. 54, no. 2, pp. 588–602, 2016.

[18] Q. Wang, J. F. L. Goosen, and F. van Keulen, "An efficient fluid-structure interaction model for optimizing twistable flapping wings," *Journal of Fluids and Structures*, vol. 73, pp. 82–99, 2017.

[19] K. Mazaheri and A. Ebrahimi, "Experimental investigation of the effect of chordwise flexibility on the aerodynamics of flapping wings in hovering flight," *Journal of Fluids and Structures*, vol. 26, no. 4, pp. 544–558, 2010.

[20] Y. Nan, M. Karásek, M. E. Lalami, and A. Preumont, "Experimental optimization of wing shape for a hummingbird-like flapping wing micro air vehicle," *Bioinspiration & Biomimetics*, vol. 12, no. 2, p. 026010, 2017.

[21] W. Shyy, H. Aono, S. K. Chimakurthi et al., "Recent progress in flapping wing aerodynamics and aeroelasticity," *Progress in Aerospace Science*, vol. 46, no. 7, pp. 284–327, 2010.

[22] Y. Nan, M. Karasek, M. Lalami, and H. Altartouri, "An experimental study on effect of wing geometry of hummingbird-like flapping wing in the hover," in *International Micro Air Vehicles Conference and Flight Competition*, Aachen, Germany, 2015.

[23] Y. J. Lee, K. B. Lua, and T. T. Lim, "Aspect ratio effects on revolving wings with rossby number consideration," *Bioinspiration & Biomimetics*, vol. 11, no. 5, 2016.

[24] Y. J. Lee, K. B. Lua, T. T. Lim, and K. S. Yeo, "A quasi-steady aerodynamic model for flapping flight with improved adaptability," *Bioinspiration & Biomimetics*, vol. 11, no. 3, 2016.

[25] Y. J. Lee and K. B. Lua, "Optimization of simple and complex pitching motions for flapping wings in hover," *AIAA Journal*, vol. 56, no. 6, pp. 2466–2470, 2018.

[26] A. Azuma, *The Biokinetics of Flying and Swimming*, Springer-Verlag, Tokyo, 1992.

[27] R. F. Chapman, *The Insects: Structure & Function*, Cambridge University Press, 1998.

[28] M. J. Lighthill, "Introduction to the Scaling of Aerial Locomotion," in *Scale Effects in Animals Locomotion*, pp. 365–404, Academic Press, London, 1977.

[29] R. Dudley, "Biomechanics of flight in neotropical butterflies: morphometrics and kinematics," *Journal of Experimental Biology*, vol. 150, pp. 37–53, 1990.

[30] D. N. Byrne, S. L. Buchmann, and H. G. Spangler, "Relationship between wing loading, wing beat frequency and body mass in homopterous insects," *Journal of Experimental Biology*, vol. 135, pp. 9–23, 1988.

[31] H. C. Corben, "Wing-beat frequencies, wing-areas and masses of flying insects and hummingbirds," *Journal of Theoretical Biology*, vol. 102, no. 4, pp. 611–623, 1983.

[32] R. D. Bullen and N. L. McKenzie, "Scaling bat wingbeat frequency and amplitude," *Journal of Experimental Biology*, vol. 205, Part 17, pp. 2615–2626, 2002.

[33] N. S. Ha, Q. T. Truong, N. S. Goo, and H. C. Park, "Relationship between wingbeat frequency and resonant frequency of the wing in insects," *Bioinspiration & Biomimetics*, vol. 8, no. 4, 2013.

[34] C. H. Greenewalt, *Hummingbirds*, Dover Publications, 1990.

[35] H. Tennekes, *The Simple Science of Flight (from Insects to Jumbo Jets)*, MIT Press, Boston, MA, 1996.

[36] W. Shyy, M. Berg, and D. Ljungqvist, "Flapping and flexible wings for biological and micro air vehicles," *Progress in Aerospace Science*, vol. 35, no. 5, pp. 455–505, 1999.

[37] R. A. Norberg and U. M. Norberg, "Take-off, landing, and flight speed during fishing flights of *Gavia stellata* (Pont.)," *Ornis Scandinavica*, vol. 2, no. 1, p. 55, 1971.

[38] R. Dudley, *The Biomechanics of Insect Flight: Form, Function, Evolution*, Princeton University Press, 2002.

[39] U. M. Norberg, "Energetics of flight," in *Avian Energetics and Nutritional Ecology*, C. Carey, Ed., pp. 199–249, Springer, Boston, MA, USA, 1996.

[40] U. M. Norberg and R. Å. Norberg, "Ecomorphology of flight and tree-trunk climbing in birds," in *Acta XIX Congressus Internationalis Ornithological*, vol. 2, pp. 2271–2282, Ottawa, Canada, 1988.

[41] U. M. Lindhe Norberg, "Structure, form, and function of flight in engineering and the living world," *Journal of Morphology*, vol. 252, no. 1, pp. 52–81, 2002.

[42] H. Oehme, "On the aerodynamics of separated primaries in the avian wing," in *Scale Effects in Animal Locomotion*, T. J. Pedley, Ed., pp. 479–494, Academic Press, London, New York, 1977.

[43] U. M. Lindhe Norberg, "Flight and scaling of flyers in nature," in *Flow Phenomena in Nature Volume 1: A Challenge to Engineering Design*, WIT Transactions on State of the Art in Science and Engineering, pp. 120–154, 2006.

[44] M. H. Dickinson, F. O. Lehmann, and S. P. Sane, "Wing rotation and the aerodynamic basis of insect flight," *Science*, vol. 284, no. 5422, pp. 1954–1960, 1999.

[45] C. P. Ellington, "The aerodynamics of hovering insect flight. II. Morphological parameters," *Philosophical Transactions of the Royal Society B: Biological Sciences*, vol. 305, no. 1122, pp. 17–40, 1984.

[46] K. B. Lua, T. T. Lim, and K. S. Yeo, "Scaling of aerodynamic forces of three-dimensional flapping wings," *AIAA Journal*, vol. 52, no. 5, pp. 1095–1101, 2014.

[47] C. H. Greenewalt, *Dimensional Relationships for Flying Animals*, vol. 144, Smithsonian Miscellaneous Collections, 1962.

[48] U. M. Norberg, *Vertebrate Flight: Mechanics, Physiology, Morphology, Ecology and Evolution*, Springer, 1990.

[49] C. Pennycuick, "Wingbeat frequency of birds in steady cruising flight: new data and improved predictions," *Journal of Experimental Biology*, vol. 199, Part 7, pp. 1613–1618, 1996.

[50] S. Ho, H. Nassef, N. Pornsinsirirak, Y. C. Tai, and C. M. Ho, "Unsteady aerodynamics and flow control for flapping wing flyers," *Progress in Aerospace Science*, vol. 39, no. 8, pp. 635–681, 2003.

[51] C. P. van Dam, K. Nikfetrat, and P. M. H. W. Vijgen, "Lift and drag calculations for wings and tails: techniques and applications," *Contemporary Mathematics*, vol. 141, pp. 463–477, 1993.

[52] W. Shyy, H. Aono, C. K. Kang, and H. Liu, *An Introduction to Flapping Wing Aerodynamics*, Cambridge University Press, New York, NY, 2013.

[53] M. T. Keennon, K. R. Klingebiel, A. Andryukov, and B. D. Hibbs, *Air Vehicle Flight Mechanism and Control Method, Aerovironment Patent*, 2010.

[54] J. K. Shang, S. A. Combes, B. M. Finio, and R. J. Wood, "Artificial insect wings of diverse morphology for flapping-wing micro air vehicles," *Bioinspiration & Biomimetics*, vol. 4, no. 3, 2009.

[55] N. S. Ha, Q. V. Nguyen, N. S. Goo, and H. C. Park, "Static and dynamic characteristics of an artificial wing mimicking an Allomyrina dichotoma beetle's hind wing for flapping-wing micro air vehicles," *Experimental Mechanics*, vol. 52, no. 9, pp. 1535–1549, 2012.

[56] W. Shyy, C. K. Kang, P. Chirarattananon, S. Ravi, and H. Liu, "Aerodynamics, sensing and control of insect-scale flapping-wing flight," *Proceedings of the Royal Society A: Mathematical, Physical and Engineering Science*, vol. 472, no. 2186, article 20150712, 2016.

[57] K. Chang, A. Chaudhuri, J. Rue et al., "Improving the fabrication process of micro-air-vehicle flapping wings," *AIAA Journal*, vol. 53, no. 10, pp. 3039–3048, 2015.

[58] Y. Chen and Y. Li, *Computational Intelligence Assisted Design: In Industrial Revolution 4.0*, CRC Press, Boca Raton, 1st Edition edition, 2018.

[59] Y. P. Liu and M. Sun, "Wing kinematics measurement and aerodynamic force and moments computation of hovering hoverfly," in *2007 1st International Conference on Bioinformatics and Biomedical Engineering*, pp. 452–455, Wuhan, China, July 2007.

[60] S. Mao and D. Gang, "Lift and power requirements of hovering insect flight," *Acta Mechanica Sinica*, vol. 19, no. 5, pp. 458–469, 2003.

[61] S. N. Fry, R. Sayaman, and M. H. Dickinson, "The aerodynamics of hovering flight in *Drosophila*," *Journal of Experimental Biology*, vol. 208, no. 12, pp. 2303–2318, 2005.

[62] A. R. Ennos, "The kinematics and aerodynamics of the free flight of some Diptera," *Journal of Experimental Biology*, vol. 142, pp. 49–85, 1989.

[63] O. Sotavalta, "The essential factor regulating the wing-stroke frequency of insects in wing mutilation and loading experiments at subatmospheric pressure," *Annales Zoologici Societatis Zoologicae Botanicae Fennicae Vanamo*, vol. 15, pp. 1–67, 1952.

[64] L. Ristroph, G. Ristroph, S. Morozova et al., "Active and passive stabilization of body pitch in insect flight," *Journal of The Royal Society Interface*, vol. 10, no. 85, article 20130237, 2013.

[65] B. Hocking, "The intrinsic range and flight speed of insects," *Transactions of the Royal Entomological Society of London*, vol. 104, pp. 223–345, 1953.

[66] R. Dudley, "Extraordinary flight performance of orchid bees (Apidae: Euglossini) hovering in heliox (80% He/20% O2)," *Journal of Experimental Biology*, vol. 198, Part 4, pp. 1065–1070, 1995.

[67] C. P. Ellington, "The aerodynamics of hovering insect flight. III. Kinematics," *Philosophical Transactions of the Royal Society B: Biological Sciences*, vol. 305, no. 1122, pp. 41–78, 1984.

[68] R. Dudley and C. P. Ellington, "Mechanics of forward flight in bumblebees: I. Kinematics and morphology," *Journal of Experimental Biology*, vol. 148, pp. 19–52, 1990.

[69] M. Okamoto, K. Yasuda, and A. Azuma, "Aerodynamic characteristics of the wings and body of a dragonfly," *Journal of Experimental Biology*, vol. 199, Part 2, pp. 281–294, 1996.

[70] M. Sato and A. Azuma, "The flight performance of a damselfly Ceriagrion melanurum Selys," *Journal of Experimental Biology*, vol. 200, Part 12, pp. 1765–1779, 1997.

[71] R. Åke Norberg, "The pterostigma of insect wings an inertial regulator of wing pitch," *Journal of Comparative Physiology*, vol. 81, no. 1, pp. 9–22, 1972.

[72] O. Sotavalta, "The effect of wing inertia on the wing-stroke frequency of moths, dragonflies and cockroach," *Annales Botanici Fennici*, vol. 20, pp. 93–101, 1954.

[73] A. Magnan, *"La locomotion chez les animaux 1," Le vol des insectes*, Hermann, Paris, 1934.

[74] B. Cheng, X. Deng, and T. L. Hedrick, "The mechanics and control of pitching manoeuvres in a freely flying hawkmoth (Manduca sexta)," *The Journal of Experimental Biology*, vol. 214, no. 24, pp. 4092–4106, 2011.

[75] A. P. Willmott and C. P. Ellington, "The mechanics of flight in the hawkmoth Manduca sexta. II. Aerodynamic consequences of kinematic and morphological variation," *Journal of Experimental Biology*, vol. 200, Part 21, pp. 2723–2745, 1997.

[76] F. T. Muijres, L. C. Johansson, M. S. Bowlin, Y. Winter, and A. Hedenström, "Comparing aerodynamic efficiency in birds and bats suggests better flight performance in birds," *PLoS One*, vol. 7, no. 5, 2012.

[77] A. Hedenstrom, L. C. Johansson, M. Wolf, R. von Busse, Y. Winter, and G. R. Spedding, "Bat flight generates complex aerodynamic tracks," *Science*, vol. 316, no. 5826, pp. 894–897, 2007.

[78] F. T. Muijres, L. C. Johansson, R. Barfield, M. Wolf, G. R. Spedding, and A. Hedenstrom, "Leading-edge vortex improves lift in slow-flying bats," *Science*, vol. 319, no. 5867, pp. 1250–1253, 2008.

[79] F. T. Muijres, L. Christoffer Johansson, Y. Winter, and A. Hedenström, "Leading edge vortices in lesser long-nosed bats occurring at slow but not fast flight speeds," *Bioinspiration & Biomimetics*, vol. 9, no. 2, article 025006, 2014.

[80] R. Bullen and N. L. McKenzie, "Bat airframe design: flight performance, stability and control in relation to foraging ecology," *Australian Journal of Zoology*, vol. 49, no. 3, pp. 235–261, 2001.

[81] N. L. McKenzie, L. Fontanini, N. V. Lindus, and M. R. Williams, "Biological inventory of Koolan Island, Western Australia 2. Zoological notes," *Records-Western Australian Museum*, vol. 17, pp. 249–266, 1995.

[82] J. H. Fullard, C. Koehler, A. Surlykke, and N. L. McKenzie, "Echolocation ecology and flight morphology of insectivorous bats (Chiroptera) in South-Western Australia," *Australian Journal of Zoology*, vol. 39, no. 4, pp. 427–438, 1991.

[83] N. L. McKenzie and J. K. Rolfe, "Structure of bat guilds in the Kimberley mangroves, Australia," *Journal of Animal Ecology*, vol. 55, no. 2, pp. 401–420, 1986.

[84] M. Thollesson and U. M. Norberg, "Moments of inertia of bat wings and body," *Journal of Experimental Biology*, vol. 158, pp. 19–35, 1991.

[85] M. J. Fernandez, *Flight Performance and Comparative Energetics of the Giant Andean Hummingbird*, PhD Thesis, University of California, Berkeley, 2010.

[86] P. Chai and D. Millard, "Flight and size constraints: hovering performance of large hummingbirds under maximal loading," *Journal of Experimental Biology*, vol. 200, Part 21, pp. 2757–2763, 1997.

[87] B. W. Tobalske, D. L. Altshuler, and D. R. Powers, "Take-off mechanics in hummingbirds (Trochilidae)," *Journal of Experimental Biology*, vol. 207, no. 8, pp. 1345–1352, 2004.

[88] D. J. Wells, "Muscle performance in hovering hummingbirds," *Journal of Experimental Biology*, vol. 178, pp. 39–57, 1993.

[89] M. Wolf, V. M. Ortega-Jimenez, and R. Dudley, "Structure of the vortex wake in hovering Anna's hummingbirds (Calypte anna)," *Proceedings of the Royal Society B: Biological Sciences*, vol. 280, no. 1773, article 20132391, 2013.

[90] D. Evangelista, M. J. Fernández, M. S. Berns, A. Hoover, and R. Dudley, "Hovering energetics and thermal balance in Anna's hummingbirds (Calypte anna)," *Physiological and Biochemical Zoology*, vol. 83, no. 3, pp. 406–413, 2010.

[91] P. Chai, R. Harrykissoon, and R. Dudley, "Hummingbird hovering performance in hyperoxic heliox: effects of body mass and sex," *Journal of Experimental Biology*, vol. 199, Part 12, pp. 2745–2755, 1996.

[92] T. Weis-Fogh, "Energetics of hovering flight in hummingbirds and in Drosophila," *Journal of Experimental Biology*, vol. 56, pp. 79–104, 1972.

[93] D. L. Altshuler, *Ecophysiology of Hummingbird Flight along Elevational Gradients: an Integrated Approach*, PhD Thesis, University Of Texas at Austin, 2001.

[94] S. Dhawan, "Bird flight," *Sadhana*, vol. 16, no. 4, pp. 275–352, 1991.

[95] A. Bontemps, T. Vanneste, J. B. Paquet, T. Dietsch, S. Grondel, and E. Cattan, "Design and performance of an insect-inspired nano air vehicle," *Smart Materials and Structures*, vol. 22, no. 1, 2013.

[96] J. A. Roll, B. Cheng, and X. Deng, "Design, fabrication, and experiments of an electromagnetic actuator for flapping wing micro air vehicles," in *2013 IEEE International Conference on Robotics and Automation*, pp. 809–815, Karlsruhe, Germany, May 2013.

[97] D. Watman and T. Furukawa, "A parametric study of flapping wing performance using a robotic flapping wing," in *2009 IEEE International Conference on Robotics and Automation*, pp. 3638–3643, Kobe, Japan, May 2009.

[98] R. Sahai, K. C. Galloway, and R. J. Wood, "Elastic element integration for improved flapping-wing micro air vehicle performance," *IEEE Transactions on Robotics*, vol. 29, no. 1, pp. 32–41, 2013.

[99] D.-K. Kim, H.-I. Kim, J.-H. Han, and K.-J. Kwon, "Experimental investigation on the aerodynamic characteristics of a bio-mimetic flapping wing with macro-fiber composites," *Journal of Intelligent Material Systems and Structures*, vol. 19, no. 3, pp. 423–431, 2007.

[100] D. Campolo, M. Azhar, G. K. Lau, and M. Sitti, "Can DC motors directly drive flapping wings at high frequency and large wing strokes?," *IEEE/ASME Transactions on Mechatronics*, vol. 19, no. 1, pp. 109–120, 2014.

[101] R. J. Wood, "Design, fabrication, and analysis of a 3DOF, 3cm flapping-wing MAV," in *2007 IEEE/RSJ International Conference on Intelligent Robots and Systems*, pp. 1576–1581, San Diego, CA, USA, October-November 2007.

[102] Q.-V. Nguyen, W. L. Chan, and M. Debiasi, "An insect-inspired flapping wing micro air vehicle with double wing clap-fling effects and capability of sustained hovering," in , Article ID 94290U*SPIE Smart Structures and Materials Nondestructive Evaluation and Health Monitoring*, vol. 9429, San Diego, CA, USA, March 2015.

[103] D. Lentink, S. R. Jongerius, and N. L. Bradshaw, "The scalable design of flapping micro-air vehicles inspired by insect flight-*Flying Insects and Robots*, D. Floreano, J. C. Zufferey, M. Srinivasan, and C. Ellington, Eds., pp. 185–205, Springer, Berlin, Heidelberg, 2009.

[104] K. Meng, W. Zhang, W. Chen et al., "The design and micromachining of an electromagnetic MEMS flapping-wing micro air vehicle," *Microsystem Technologies*, vol. 18, no. 1, pp. 127–136, 2012.

[105] H. Tanaka and R. J. Wood, "Fabrication of corrugated artificial insect wings using laser micromachined molds," *Journal of Micromechanics and Microengineering*, vol. 20, no. 7, 2010.

[106] K. Y. Ma, P. Chirarattananon, S. B. Fuller, and R. J. Wood, "Controlled flight of a biologically inspired, insect-scale robot," *Science*, vol. 340, no. 6132, pp. 603–607, 2013.

[107] T. N. Pornsin-Sirirak, Y.-C. Tai, C.-M. Ho, and M. Keennon, "Microbat: a palm-sized electrically powered ornithopter," in *Proceedings of NASA/JPL Workshop on Biomorphic Robotics*, pp. 14–17, Pasadena, CA, USA, August 2001.

[108] H. Tanaka, H. Okada, Y. Shimasue, and H. Liu, "Flexible flapping wings with self-organized microwrinkles," *Bioinspiration & Biomimetics*, vol. 10, no. 4, 2015.